Biomaterials Science

ROYAL SOCIETY OF CHEMISTRY

REVIEW

View Article Online
View Journal

Cite this: DOI: 10.1039/d6bm00661b

Towards supramolecular regenerative medicine using low-molecular-weight gelator hydrogels for stem cell growth

Chayanan Tangsombun[a,b] and David K. Smith *[a]

This review explores gels that assemble from low-molecular-weight gelator (LMWG) building blocks for use in cell culture, with a focus on fibroblasts and stem cells. These LMWG hydrogels have unique potential for controlling and directing cell growth. We provide an overview of gel tunability and how careful molecular design can direct biological outcomes. The LMWG hydrogel approach to cell growth is based on reversible assembly, potentially enabling cells to be encapsulated and subsequently released. It is possible to easily formulate multiple active ingredients into LMWG hydrogels by co-assembly – a powerful strategy to create multi-functional hybrid hydrogels. Rheological properties can be tuned over orders of magnitude, with stiffness helping control properties like cell invasion or stem cell differentiation. Furthermore, gel dynamics at both molecular and network levels can control factors such as cell adhesion. By developing strategies to shape and pattern these gels, it is possible to create structured assemblies of cells or direct the growth of multi-functional biological tissues. The dynamic characteristics of these gels enables them to evolve, potentially facilitating 4D tissue engineering or the creation of materials that are both bio-instructive and bio-responsive. LMWG hydrogels have been applied both *in vitro* and *in vivo* and some are in commercial use. This critical review provides an overview of progress to date, emphasising the unique advantages of the LMWG hydrogel approach, and highlighting concepts that might unlock untapped potential, hence transforming next-generation regenerative medicine.

Received 28th April 2026,
Accepted 9th June 2026

DOI: 10.1039/d6bm00661b

rsc.li/biomaterials-science

[a]*Department of Chemistry, University of York, Heslington, York, YO10 5DD, UK. E-mail: david.smith@york.ac.uk*
[b]*Department of Materials Science and Engineering, School of Molecular Science and Engineering, Vidyasirimedhi Institute of Science and Technology (VISTEC), Rayong, 21210, Thailand*

Chayanan Tangsombun

Dr Chayanan Tangsombun completed her PhD in Chemistry at the University of York under the supervision of Prof. David K. Smith, where her research focused on low-molecular-weight gelator hydrogels and patterned soft materials for biomedical applications, including multi-component gels, reaction–diffusion patterning, gold nanoparticle-loaded materials, and biocompatible gels for directing mesenchymal stem cell growth. She is currently a Postdoctoral Researcher at the Vidyasirimedhi Institute of Science and Technology (VISTEC), Thailand.

David K. Smith

David Smith was educated at the University of Oxford, carried out postdoctoral research at ETH Zurich and has been an academic at University of York since 1999. In recognition of his research team's work on LMWG hydrogels, he was awarded the prestigious RSC 'Tilden Prize'. He also received the SCI 'Science for Society Award' for chemical education and outreach. Dave has engaged extensively on wide-ranging aspects of inclusion and diversity, being named on Attitude Magazine's '101 List' of influential LGBT + figures (2026). Since the death of his husband in 2019, Dave has worked part-time and is a single parent to their son.

1. Introduction

1.1 Introduction to LMWG hydrogels for tissue engineering

Hydrogels are colloidal soft materials in which a solid-like network extends through a bulk liquid-like phase, effectively immobilising it.[1] Having solid-like and liquid-like characteristics, wide-ranging mechanical properties, and the potential for chemical modification and/or encapsulation of bioactive agents, hydrogels are well-placed to mimic key aspects of the extracellular matrix, and there is therefore considerable interest in using such materials to support cell growth.[2] There are a number of ways a hydrogel matrix can interact with growing cells, which are explored throughout this article.

A variety of different classes of hydrogel are known, with polymer hydrogels being best-established.[3] The solid-like 3D network of a polymer gels is achieved *via* interactions between polymeric gelators – covalent cross-linking gives rise to a chemical gel, non-covalent interactions result in physical gels. Hydrogels based on polymers such as collagen, alginate, or hyaluronic acid have natural origins, while those based on polymers such as poly(lactic acid) or poly(ethylene glycol) are synthetic. Although natural and synthetic polymers are widely used for cell culture, there remains a need to control disassembly and degradation, enhance cell adhesion, and further enable their controlled modification.[4]

A second class of hydrogel of primary interest here, employs low-molecular-weight gelators (LMWGs, Fig. 1).[5] LMWGs are well-defined molecular species with molecular masses typically ≤1000 Da. They are held together *via* reversible non-covalent interactions such as hydrogen bonds, ionic interactions, π–π interactions, van der Waals forces, and the hydrophobic effect, which result in their self-assembly into fibrils (supramolecular polymers). These fibrils interact with one another, usually *via* a bundling mechanism, to form nanoscale fibres. These fibres interact and entangle to establish a sample-spanning network that traps solvent, resulting in gelation. All levels of hierarchical assembly in these materials are controlled by non-covalent interactions. Such materials are often simply referred to as 'supramolecular gels', however, this term is also sometimes used in the literature to refer to gels formed from much larger polymers, held together by supramolecular interactions – as such it can introduce ambiguity.[6] In this review, we therefore refer to the gels of interest as 'LMWG hydrogels' – *i.e.* the LMWG can assemble into a gel without need of a polymeric component. LMWG hydrogels have been used as biomaterials for cell culture and tissue engineering, and a number of reviews have been published.[7,8] As highlighted by Dankers and co-workers,[9] gels that incorporate supramolecular components are uniquely well placed to exhibit controlled mechanics and dynamics that can directly impact on cell growth outcomes. LMWG hydrogels are stimulus-responsive materials with high water content, adaptability, biodegradability, potential biocompatibility and tuneable physiochemical properties, which can mimic extracellular matrix. They allow the diffusion and transportation of small molecules, nutrients and oxygen and can incorporate biochemical cues in a variety of ways to regulate stem cell behaviour.

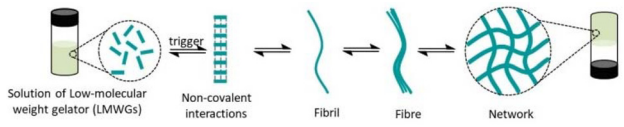

Fig. 1 Schematic illustration of the hierarchical self-assembly of a LMWG-based gel *via* non-covalent interactions to form fibrils that bundle into fibres that constitute a sample-spanning gel-phase network.

There is increasing focus on regenerative medicine enabling new modalities of disease treatment. *In vivo* repair of damaged tissue is of high value in a clinical setting, while *ex vivo* development of replacement tissue for later implantation holds the potential of transforming the treatment of diseased or damaged organs.[10] The understanding of stem cells (see section 1.2) has enabled this research, and controlling stem cell growth has become a vital frontier in the development of next generation medical technology. In this review, we explore a broad range of LMWG hydrogels and develop insights into their ability to support and direct cell growth (Fig. 2). Different types of cell have unique requirements and sensitivities that impact on their growth on hydrogel supports.[11] We primarily focus attention on stem cells (and to a lesser extent fibroblasts), as these cell types have the most wide-ranging potential in regenerative medicine.

1.2 Introduction to cell types

Stem cells have the potential to self-renew and differentiate to different types of cell in response to specific stimuli. They can be divided into two main categories – embryonic and adult.[12] Adult stem cells were first isolated from bone marrow by Friedenstein in the 1960s.[13,14] In 1998, human embryonic stem cells were first isolated by Thomson and co-workers, and their potential therapeutic use was discussed.[15] However, the use of embryonic stem cells raises significant ethical considerations, which can make adult stem cells more suitable for fundamental research and clinical applications.[16] In 2007, Thomson and co-workers isolated human induced pluripotent stem cells (hiPSCs) from human somatic cells, and demonstrated they exhibit the same essential characteristics as embryonic stem cells. Adult stem cells can be isolated from a variety of accessible sources such as adipose tissue, nerve tissue, and skin,[17] and different types of stem cell can differentiate into different types of mature cell. For example, mesenchymal stem/stomal cells (MSCs) differentiate into fat (adipogenesis), cartilage (chondrogenesis) or bone (osteogenesis) cells, and can be engineered to stimulate tissue repair.[18]

The fact stem cells can be isolated from patients means using them to generate tissues for implantation can be done in a personalised way, potentially avoiding waiting for a donor, as well as problems with rejection that otherwise persist long after implantation.[19] Given the transformative potential of this approach to medicine, many methods have been investigated

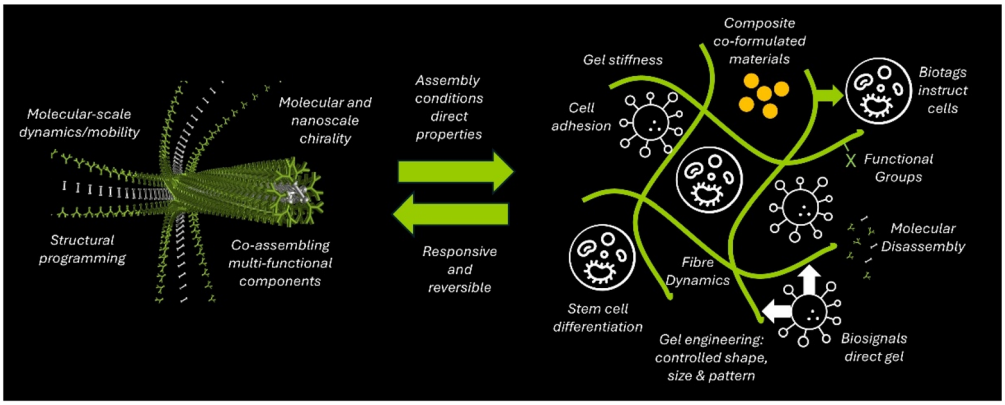

Fig. 2 Schematic diagram exploring the benefits of LMWG hydrogels, highlighting how they can interface with growing cellular tissue to direct biological outcomes.

to regulate cell proliferation and differentiation, and activity in this field of research is intense.

Combining stem cells with hydrogel scaffolds offers space for new tissue to form and the opportunity to engineer the structure of the resulting tissue.[20] The vast majority of research has used polymer hydrogels, but there is significant and growing interest in the design and development of LMWG hydrogels for cell-growth. As described above, such materials offer advantages of being reversible, easily synthetically modified, readily tuned in terms of their materials properties, and easily combined to form multi-component materials.

In addition to stem cells, it is also worth considering human umbilical vein endothelial cells (HUVECs). Although they are not stem cells, they can be reprogrammed into induced pluripotent stem cells, and have significant uses in regenerative medicine – selected examples in this review therefore make use of HUVECs.

Fibroblasts are also of key interest in regenerative medicine.[21,22] They are mostly found in connective tissue, have a spindle-shaped morphology and can generate and maintain extracellular matrix, as well as providing structural support for tissues and organs. When injury occurs, fibroblasts are activated and migrate to the wound site. They are intimately involved in key processes in wound healing and tissue regeneration.[23] Fibroblasts are sometimes considered an alternative to MSCs as they have similar characteristics like surface markers and differentiation potential.[24,25] They can be directly obtained from tissues, and have a high rate of proliferation, which reduces time and cost for cell culturing, making them easier to work with than stem cells and less sensitive to culture conditions. However, their potential scope of application is not as broad as stem cells. This review includes selected examples of fibroblast growth on LMWG hydrogels to emphasise key themes.

Many cell-based studies of LMWG hydrogels have explored the growth of cancer cell lines. Cancer cells are generally much easier to culture than stem cells or fibroblasts because of their dysregulated reproduction. Many studies of LMWG hydrogels in combination with cancer have focused on preventing cancer cell growth and are thematically far removed from regenerative medicine. However, we will briefly mention a few examples where cancer cells have been deliberately cultured on LMWG hydrogels that emphasise important principles.

2. Gelator structures

A key advantage of LMWG hydrogels is the high degree of structural variability that can be introduced into the LMWG *via* simple synthetic chemistry. This introduces vast tunability and the potential to use molecular structure to control materials properties, and cell growth outcomes.

2.1 Origins – hydrogels based on larger peptides (M_n > 1000)

In pioneering work at the origins of the field, 1995 saw Zhang and co-workers report a peptide hydrogel based on self-complementary peptides with repeating motifs of alternating hydrophilic and hydrophobic amino acids, which associated to form stable β-sheets in water.[26] The addition of buffers containing millimolar amounts of monovalent salts, or the transfer of a peptide solution into physiological solutions, resulted in spontaneous assembly of a stable gel. Mammalian cells, including cancer cells and fibroblasts, could attach themselves to these gel scaffolds. In 2000, the same researchers reported a peptide-based hydrogel with four arginine, alanine, aspartate and alanine (RADA) repeat units for the growth of primary neuronal cells.[27] Although not culturing stem cells, this early work was foundational. The $(RADA)_4$ peptide 16-mer (Fig. 3a) self-assembles into sheets because of self-complementary electrostatic interactions between positively charged arginine and negatively charged aspartate. With a molecular mass of 1712.8 Da, this LMWG is above the upper threshold of what might be considered an LMWG, but neither is it really a polymer. Zhang and co-workers demonstrated that the nanofibrillar hydrogel (Fig. 3b) encouraged neuronal cell attachment and differentiation, extensive neurite outgrowth and the formation of functional synapses *in vitro*. In a landmark 2005 study, they went on to demonstrate that injecting this LMWG into the damaged optic nerve of hamsters supported axon regeneration (Fig. 3c

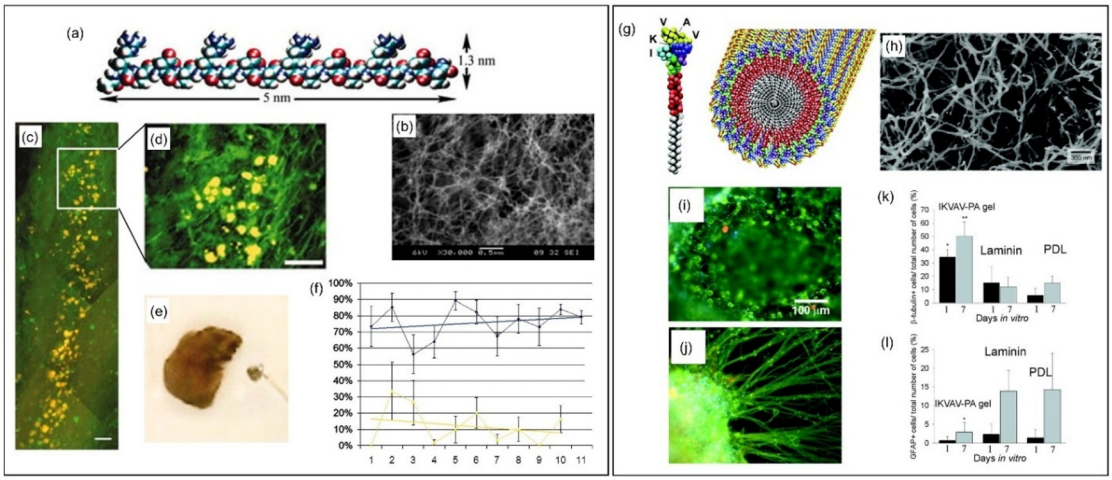

Fig. 3 Left box: (a) Molecular model of the RADA16-I molecular building block. (b) SEM image of self-assembled gel (scale bar, 500 nm). (c) Dark-field photo of a parasagittal section from the brain of an 8-month old hamster treated with gel at the time of surgery in the lesion site. The yellow dots show the location of the lesion. The axons, shown by green fluorescence, have grown through the site of lesion without tissue disruption. (d) Enlargement showing dense regenerated axons, in green, through the lesion site. (e) Photograph of gel-treated adult hamster turning toward visual stimulus in the damaged right visual field. (f) Graph showing percentage response of animals when a visual stimulus was presented to the eye connected to the treated optic tract (blue) or spontaneous turns of blind animals of the control group (yellow) – testing was done in sessions starting 6 weeks after surgery. Right box: (g) Molecular model of IKVAV-PA showing its assembly into a cylindrical micelle. (h) SEM image of IKVAV-PA gel (scale bar 300 nm). (i) NPCs encapsulated in IKVAV-PA gels at 1 day with differentiated neurons labelled in green, and astrocytes labelled in orange. (j) NPC neurosphere encapsulated in an IKVAV-PA nanofiber network at 7 days with a large extent of neurite outgrowth. (k) Percentage of total cells that differentiated into neurons (β-tubulin+). The IKVAV-PA gels had significantly more neurons compared to both laminin and poly-D-lysine (PDL) controls. (l) Percentage of total cells that differentiated into astrocytes (GFAP+). The IKVAV-PA gels had significantly fewer astrocytes compared to both laminin and PDL controls. Figure adapted from ref. 28 and 29 with permission of the National Academy of Sciences, copyright 2006, and Science, copyright 2004, respectively.

and d) and stimulated the return of functional vision *in vivo* (Fig. 3e and f).[28]

In 2006, moving beyond these initial studies, which used primary neuronal cells, Zhang and co-workers combined their RADA-based gelator with adult mouse neural stem cells, and explored its potential for 3D tissue culture.[30] They further modified the peptide by grafting-on sequences associated with cell adhesion, such as RGD, YIGSR, IKVAV *etc*. Although increasing complexity, this did not adversely affect the self-assembly of gel nanofibres. While the standard RADA peptide gel could support stem cell proliferation, cell growth was significantly better on gels modified with adhesion motifs, reflecting the relative challenge associated with culturing stem cells. Differentiation of stem cells into neurons was also improved. Cell growth was benchmarked against Matrigel, a widely used animal-extract extracellular matrix mimic – the self-assembling peptides were competitive with Matrigel. Others have modified RADA peptides with similar results.[31] A number of other researchers have also developed β-sheet forming peptide hydrogels,[32,33] but given these again have molecular masses >1000 Da, we do not provide full details here.

This early work indicated that synthetic gel matrices had potential to replace bioderived materials when working with stem cells,[34] offering advantages of greater reproducibility, ease of manufacture and avoidance of ethical issues associated with animal-derived products. RADA-based gels have been commercialised as 'PuraMatrix®' for use in laboratory research and 'PuraStat®' for use in a surgical setting as a hemostatic (blood clotting) agent.[35,36] These are relatively rare examples of non-polymeric hydrogels that have transitioned from an academic laboratory into commercial use. As limitations, it is worth noting that it is typically necessary to mix bioactive units into the gels to optimise cell growth. Synthetic limitations mean the peptide is only sold at a purity of >90% and has relatively high cost (>$100 per 10 mg) – there is therefore significant scope for simpler LMWGs to have a commercial impact.

Contemporary with Zhang and co-workers, Stupp's research team were working on self-assembling peptides, with a design philosophy more inspired by surfactant chemistry than protein science. Peptide amphiphiles (PAs) were developed, which have block-like structures, with hydrophobic and hydrophilic domains.[37] These PAs assemble into cylindrical micelles, which, if they have 'sticky' surfaces, yield sample-spanning gels *via* micelle–micelle interactions. In 2004, Stupp and co-workers cultured neural progenitor cells (a more specialised descendent of neural stem cells that do not have the capacity to replicate indefinitely) on a PA scaffold that incorporated IKVAV (isoleucine-lysine-valine-alanine-valine), known to promote neurite formation (Fig. 3g).[29] The nanofibre scaffold (Fig. 3h) induced rapid differentiation of progenitor cells into neurons, while discouraging astrocyte development, and it was argued that the multivalent presentation of bioactive IKVAV to

the stem cells on the self-assembled nanofibres was responsible for this selective differentiation (Fig. 3i–k). The molecular mass of this PA (*ca.* 1200 Da) means it is above the threshold of what may be considered a true LMWG, but the ability to precisely control chemical structure clearly differentiates PAs from polymeric systems, and instructive key principles emerge from this work.

In 2008, Stupp and co-workers used this scaffold to treat spinal cord injury.[38] The PA assembled to form a gel in the presence of cations, and the gelator solution was injected to the extracellular environment of spinal cord, giving self-assembled nanofibers *in vivo*. With neural stem cells, glial differentiation and scar formation was inhibited while neurite extension was supported. A mouse model with a spinal cord injury was investigated, and animals injected with the hydrogel had greater locomotor scores than those receiving a placebo glucose injection, indicating the assembled PA hydrogel promoted tissue regeneration. It was also reported that the IKVAV hydrogel supported proliferation of human embryonic stem cells *in vitro* and *in vivo* in the inner ear.[39] It was suggested this may be useful in regeneration of the spiral ganglion.

In recent years, AmphixBio has been commercialising PA systems developed by Stupp and co-workers, with particular focus on innovative treatments for acute spinal cord injury (SCI). The aim is to combine the nanofiber scaffold with the pharmacological action of peptide drugs in a single therapy. SCI is experienced by *ca.* 500 000 people a year globally, many at a relatively young age, and given the lack of current therapies, there is potential for these self-assembling systems to transform clinical practice.

Protein chemists have developed other approaches to hydrogels using larger peptides. For example, 'coiled coils' contain relatively long α-helical peptides (*ca.* 20+ repeat units), which can be designed to mutually interact and hence bundle into coiled fibres, that underpin gels.[40] Such gels can be programmed at the amino acid level. Although these peptides are monodisperse, well-defined molecules, they exceed the threshold of what could reasonably be considered 'low-molecular-weight' gelators. As such, we refer the interested reader to work exploring their stem cell engineering potential.[41]

2.2 Ultra-short peptide hydrogels for cell growth

As discussed above, larger peptides have application as cell growth matrices, both academically and commercially. However, they are relatively large molecules (M_n > 1000) that require iterative peptide synthesis. Although the process can, in part, be automated, it nonetheless comes at a significant financial cost of reagents/solvents and imposes some inherent limitations on scale. Although it might be argued that relatively high costs are standard in biomedical science, it is also highly desirable for the costs to fall, in order to democratise access to the technology and limit barriers to entry for scientists in developing economies. Furthermore, the extensive but necessary use of protecting groups in peptide synthesis is not particularly sustainable. There are therefore genuine advantages in using truly low-molecular-weight systems with M_n < 1000 that can be easily synthesised *via* short sequences of low-cost, scalable, sustainable reactions. As such there has been significant interest in 'ultrashort peptides' that assemble into LMWG hydrogels with potential to support cell growth.

Gazit and co-workers first noted short aromatic dipeptides could assemble into nanostructures as a result of π–π stacking,[42,43] and Xu and co-workers went on to report that the presence of an Fmoc protecting group promoted assembly,[44,45] In 2006, Ulijn and co-workers reported the Fmoc-protected diphenylalanine peptide (**Fmoc-FF**, Fig. 4) as an effective low-molecular-weight hydrogelator.[46] This LMWG combines hydrophilic hydrogen bonding peptides and hydrophobic π-stacking groups – it has since become a privileged and popular LMWG.[47] Even in their earliest report,[46] Ulijn and co-workers recognised the potential of this simple LMWG as a cell-growth scaffold. Specifically, they cultured phenotype bovine chondrocytes and demonstrated cytocompatibility, with both 2D culture (on the gel) and 3D culture (in the gel) being possible, albeit with limited proliferation. In 2007, Liebmann and co-workers also explored **Fmoc-FF** as a potential scaffold for mammalian cell culture.[48] Although not using stem cells, they used fibroblasts. Microscopy revealed that cells suspended in these hydrogels tended to adopt 3D structures, rather than the elongated conformations seen for 2D surface cultures. They also demonstrated, at least in preliminary studies, a degree of reversibility of these self-assembled gels. This is a key potential advantage of the LMWG approach as it opens the possibility of disassembly-on-demand to release cultured cells/tissue (see section 6.3.1).

More recently, an interesting study from Azarpira and co-workers compared the growth of different cell types on a related **Fmoc-FV** hydrogel (Fig. 4).[49] Endothelial cells and a breast cancer cell line were more viable in the gel than mesenchymal stem cells, demonstrating the relative sensitivity of stem cells. The authors suggested one of the problems was poor adhesion between stem cells and the dipeptide hydrogel. Indeed, the importance of adhesion motifs was well-known from the early work on larger peptide gels described above. Ulijn and co-workers had also recognised this problem in their

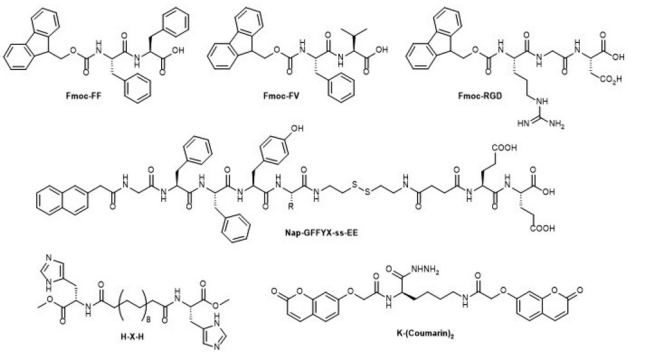

Fig. 4 Selected chemical structures of short peptides applied as LMWGs.

pioneering work on ultra-short peptide hydrogels[46] and had developed a powerful co-assembly solution (see section 2.4.1).

With a specific interest in the impact of peptide adhesion motifs, and focussing on the integrin-binding RGD motif, Hamley and co-workers compared **Fmoc-RGD** (Fig. 4) and **Fmoc-GRD**.[50] These two peptides both self-assemble to form gels with similar morphologies and mechanical strengths, but cell culture experiments revealed that while the **Fmoc-RGD** hydrogel could sustain bovine fibroblasts, **Fmoc-GRD** could not, proving that the correct sequence of amino acids was required for biological activity. This indicates how peptide design can endow LMWG hydrogels with bioactivity – indeed, the exquisite chemical variability of amino acids is a key advantage of peptide LMWGs.

Further demonstrating the tunability of peptide hydrogels, Martin, Thordarson and co-workers explored LMWGs that contained two lysines and two phenylalanines in different positions.[51] They found a degree of sequence control over the growth of primary neuronal cells, with Fmoc-FKKF and Fmoc-KFFK showing decreased neuronal viability. The other four combinations of F/K amino acids all gave good neuronal cell viability. The researchers argued that enhanced mobility of the hydrophobic residues in the two ineffective LMWGs allowed them to interact with cell membranes, causing the decreased viability. It was concluded that the precise geometric presentation of hydrophobic and hydrophilic residues may be important in modulating cell compatibility. Although not using stem cells, this study demonstrates the importance of developing a structure–activity relationship understanding of LMWG hydrogels, and hints at the importance of dynamics in gels, a topic we return to later (see section 3.2).

Hauser and co-workers also explored the impact of peptide sequence, designing two tetrapeptide hydrogels, FIIK and FFIK, with just a single amino acid difference, for culturing human dermal fibroblasts (HDF).[52] The FFIK hydrogel had significantly higher stiffness and resistance to stain than FIIK, indicating how peptide sequence can direct rheological performance. The increased stiffness is result of the greater hydrophobicity of the FFIK gel which replaces isoleucine with phenylalanine, reinforcing self-assembly. Both hydrogels were cytocompatible with fibroblasts, but later in this review we will explore examples in which tuning mechanical performance impacts significantly on cell growth (see section 3.1).

Lampe and co-workers reported pentapeptides that assembled into nanofibre gels suitable for tissue engineering, with shear thinning and rapid self-healing.[53] Their approach was based on varying a KYFIL design, and by doing this, rheological performance could be tuned over a very large range (G' = 50–17000 Pa). Working with oligodendrocyte precursor cells (OPCs), they showed that gels based on AYFIL (G' = 1900 Pa, 1.5% wt/vol) led to good cell growth, whereas KYFIL (8000 Pa, 1.5% wt/vol) resulted in poor viability. It was argued that the AYFIL gel had rheological properties that were closer to the native tissue for OPCs.

Yang and co-workers reported disulfide-based peptidic hydrogels which had a difference at just one of their amino acids, incorporating either glutamic acid, lysine or serine (**Nap-GFFYX-ss-EE**, Fig. 4).[54] Addition of glutathione reduced the disulfide, removing the hydrophilic head group, reducing solubility, and initiating gel formation in serum-free media. This provides a good example of how LMWG assembly can be triggered through careful chemical design. Modifying the amino acid changed hydrogel fibre size and mechanical stiffness. All hydrogels could encapsulate mouse fibroblast 3T3 cells, which proliferated and spread more effectively in softer hydrogels than stiffer ones.

Yuan and co-workers reported a bolaamphiphile peptide hydrogelator based on histidine methyl esters (**H-X-H**, Fig. 4).[55] Histidine endows the gel with an alternative triggering mechanism. On addition of copper(II) followed by heating, the solution changed colour from white to blue as histidine-based metal coordination occurred, and on cooling, hydrogels were formed. There was an increase in mechanical stiffness on increasing copper(II) concentration due to greater cross-linking of the gel network. The hydrogel had self-healing properties, antibacterial capability and was cytocompatible with fibroblasts. *In vivo* studies revealed that the hydrogel could encourage tissue regeneration and treat diabetic wounds.

Building on a very simple amino acid scaffold, it is possible to incorporate a number of modifications to potentially introduce functionality. As just one example, Gu and co-workers designed a lysine acylhydrazide hydrogelator that incorporated 7-carboxyl methoxycoumarin (**K-(Coumarin)$_2$**, Fig. 4).[56] Ultrasound tiggered the rapid assembly of this LMWG into nanofiber networks, accelerating gelation. To study toxicity, NIH 3T3 fibroblasts were seeded onto the gel, with the authors reporting that cells grew well and migrated inside the hydrogel.

In the chemical space between the ultra-short peptide LMWGs described above and larger peptides such as those in section 2.1, medium-sized peptides have also been explored. Kong and co-workers developed octapeptide hydrogelators incorporating a key peptide motif from collagen that was expanded with different amino acid sequences.[57] Four of the gels were non-toxic to mouse fibroblast NIH 3T3 cells, while the other two showed toxicity. The authors concluded that peptide conformation and sequence could have profound effects on cell culture – self-assembling peptides cannot simply be assumed to be non-toxic. There has also been interest in intermediate-sized peptidic hydrogels for therapeutic use – for example, Nap-GDFDFpDY with encapsulated gingiva-derived mesenchymal stem cells was used to treat radiation-induced skin wounds in a mouse model.[58]

Miller and co-workers developed octapeptide hydrogelators for use in stem cell growth.[59] Their design concept gave the peptide hydrophobic and hydrophilic faces to drive assembly, forming a β-sheet nanofiber hydrogel rather like the early work of Zhang and co-workers, only using smaller peptides that are more potent LMWGs. Human mesenchymal stem cells (hMSCs) encapsulated into this hydrogel were viable and proliferative for 3D cell culture. Rounded cells were observed, reflecting a 3D-environment with no specific adhesion points.

When using osteogenic media to help direct hMSCs, the expression of collagen-I, osteocalcin and alkaline phosphatase was detected, and mineralization of hydroxyapatite, a bone component, occurred. This indicated cell differentiation into osteoblasts; it was suggested the gel may, in combination with the right stimuli, be useful for bone regeneration. The authors also noted that the peptide hydrogel was degraded, both by components of serum, but also by cells themselves, as a result of proteolytic breakdown of the peptide bonds. This can be advantageous in terms of non-persistence of the scaffold. However, LMWG degradation can also limit longer-term cell culture, and can be a significant problem for L-peptide-based gels (see section 4).

Miller and co-workers commercialized their octapeptide gel platform technology, named 'PeptiGel'. The tunability of amino acids allowed them to create a range of PeptiGels, *e.g.* positively charged, negatively charged and neutral. It is argued this allows optimal LMWGs to be developed for specific cell types. A number of academic studies using these gels have explored compatibility of various PeptiGels with different cell lines.[60,61] In a landmark study, human induced pluripotent stem cells were used to create kidney organoids.[62] Maturation within the self-assembled 3D microenvironment significantly reduced off-target cell types, which are a known limitation of current kidney organoid protocols.

2.3 Beyond peptide hydrogels for cell culture

Although peptides are versatile and biocompatible systems, as described above, their susceptibility to proteolysis can be a disadvantage in terms of application. Furthermore, their stepwise iterative synthesis, although easily controlled and with potential for automation, can be costly in terms of reagents and sustainability. As such, there is considerable interest in alternative LMWGs for tissue engineering. This can also introduce new types of behaviour, not easily accessible for peptide hydrogels.

2.3.1 Nucleobase hydrogels. Nucleobase hydrogelators have been known since it was recognised over 100 years ago that guanosine could assemble into hydrogen-bonded G-quartets that subsequently assembled into fibrils.[63,64] The hydrogen bonding potential of nucleobases opens extensive possibilities for gel assembly. However, the use of nucleobase LMWGs in tissue culture is relatively recent.

In 2012, Chassande, Barthélemy and co-workers reported a glycosyl-nucleoside fluorinated LMWG (**GNF**, Fig. 5),[65] with a central nucleoside flanked with a fluorinated chain and a sugar (see section 2.3.2 for sugars as LMWGs). Gel formation was induced as a result of its surfactant-like characteristics *via* a heat-cool cycle, with cells being mixed into the system during cooling. This gel was injectable and degradable, but the mechanism of degradation could not unambiguously be concluded. Pleasingly, the **GNF** hydrogel was non-toxic against stem cells derived from adipose tissue for both 2D and 3D cell culture. The authors noted that in the gel, these cells differentiated to osteoblasts *in vivo* without the need for specific osteogenic induction, and that cells embedded within the gel could be easily injected to a desired implantation site.

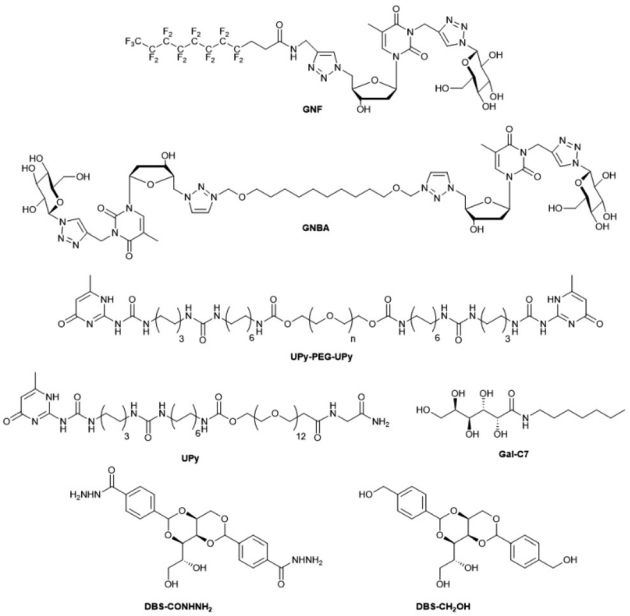

Fig. 5 Selected chemical structures of LMWGs based on nucleobases and sugars.

In a landmark study, Barthélemy and co-workers later went on to use the same nucleosidic head group to create a glycosyl-nucleoside bola-amphiphile (**GNBA**, Fig. 5).[66] The use of bola-amphiphile structures as LMWGs is a well-established general strategy in supramolecular science.[67] **GNBA** overcame some of the rheological limitations of **GNF**, with the hydrogel being significantly stiffer (G' = 30325 Pa *vs.* 1750 Pa). Pleasingly, it had thixotropic properties making it fully injectable and it was cytocompatible towards hMSCs derived from adipose tissue. The significance of the rheological tuning of these gels is explored further in section 3.1.

Dankers, Meijer and co-workers have made elegant and extensive use of a supramolecular approach to hydrogels based on ureido-pyrimidinones (**UPy**, Fig. 5).[68–70] These assemble into dimers as a result of quadruple hydrogen bonding between nucleoside head groups, while the urea groups allow for lateral aggregation of the assembled structures. Careful structural tuning includes incorporation of hydrophobic groups around the hydrogen bonding urea groups to shield them, and functionalisation with PEG chains to provide enhanced water compatibility. The addition of a bis-functionalised **UPy** derivative (**UPy-PEG-UPy**, Fig. 5) offers an additional degree of 'supramolecular polymerisation', leading to gels in which the mechanical and dynamic properties can be tuned by changing the monomer–dimer ratio. This type of supramolecular polymer is conceptually a little different to strict small molecule LMWGs, but it has generated tunable, dynamic hydrogels that exhibit exquisite control over cell growth – instructive examples of some of the principles learned are described in more detail later in this article.

2.3.2 Sugar hydrogels. Sugars are water-soluble, biocompatible materials that are highly tunable, with naturally occurring

sugars displaying a wide range of chain lengths and chiralities. Furthermore, although they do not have the functional group diversity of amino acids, they can be easily modified to create a range of derivatives. Sugar-based LMWG hydrogels have been reported in many studies – indeed, knowledge of sorbitol-based gels dates to the late 19th century.[71]

In 2018, Fitremann and co-workers simplified sugar-amphiphile design principles to the absolute minimum, creating alkylgalactonamide-based LMWGs; low-cost sugar amphiphiles that could be synthesised on multigram-scale, in a single step, with purification by recrystallisation.[72] In biological studies, heptyl galactonamide (**GalC7**, Fig. 5) led to more viable neuronal cells compared to GalC8, indicating that a structural difference of just one carbon atom on an alkyl chain can impact on biocompatibility. In terms of mechanical properties, the **GalC7** hydrogel had a low storage modulus suitable for 3D growth and differentiation of human neuronal stem cells. In addition, **GalC7** was used to culture mouse embryonic hippocampal stem cells, with high levels of expression of transcription factors Sox8, Sox9 and Sox10.[73] The high level of Sox10 indicated higher development of oligodendrocytes. There was also an interesting level of expression of Neurod1, a marker of neuronal differentiation.

When using **GalC7**, Fitremann and co-workers found the gel slightly dissolved in the cell culture media, and could not be used for extended periods (>1 week).[72] By extending the alkyl chain even further (GalC9), Fitremann and co-workers enhanced the performance for long-term cell culture.[74] However, a co-solvent (hexafluoroisopropanol, HFIP) was now required to prepare the gel – this was removed prior to cell culture. Primary dermal fibroblasts formed cell clusters with elongated and multidirectional shapes, guided by the fibers. GalC9 maintained mechanical strength for >3 weeks, although penetration of cells into the gel was somewhat limited.

Taking a different approach to minimalistic sugar-based hydrogelators, we developed LMWGs based on a 1,3:2,4-dibenzylidenesorbitol (DBS) scaffold. DBS has been established as an organogelator for well over 100 years, and is synthesised on bulk scale by the chemical industry *via* condensation of sorbitol with two equivalents of benzaldehyde.[75] It is a 'butterfly' surfactant that assembles due to hydrogen bonds between sorbitol 'bodies' and π–π stacking/solvophobicity between aromatic 'wings'. However, DBS does not form gels in pure water, and we thus targeted slightly more hydrophilic derivatives to extend gelation into this key solvent.[75] The system modified with acyl hydrazides on the aromatic 'wings' (**DBS-CONHNH$_2$**, Fig. 5), which can be synthesised in two simple, scalable steps,[76] has been of particularly high value.

In 2018, we demonstrated the viability of mouse embryonic fibroblasts on **DBS-CONHNH$_2$** hydrogels – they proliferated well, a process further enhanced by loading the growth factor promoter heparin into the gels.[77] More recently, we have demonstrated **DBS-CONHNH$_2$** has excellent compatibility with immortalised Y201 human mesenchymal stem cells (hMSCs).[78] The gels are relatively soft (G' = 600 Pa, 0.3% wt/vol) and as a result, cells loaded onto the surface can invade the matrix, retaining rounded cell shapes that remain stable over extended periods of time. Very recently, we reported a new DBS derivative, **DBS-CH$_2$OH** (Fig. 5), which also has excellent compatibility with Y201 hMSCs.[79] In contrast to **DBS-CONHNH$_2$**, the stem cells grew with spread morphologies indicative of significantly greater adhesion to the gel network and suggesting much greater potential for differentiation to bone cells. This is described in more detail in section 3.2 but clearly demonstrates how even small changes in LMWG structure can lead to significant and unpredictable differences in stem cell growth. Indeed, there is an urgent need for a greater predictive sense of understanding of the interface between LMWG hydrogels and stem cells such that gels can be designed from first principles to have the desired properties with regards to stem cell growth.[9]

2.3.3 Combining different bio-derived motifs in LMWGs. Many researchers have combined different building blocks in a single LMWG. This has the potential to introduce new assembly pathways, as well as embedding additional tunability and functionality. For example, the **GNF** described in section 2.3.1 combined a nucleoside to drive hydrogen bonded self-assembly, with a hydrophilic sugar head group within its amphiphilic structure. Taking a related approach, Xu and co-workers reported LMWGs combining nucleobase, amino acid and saccharide units into a single 'NAS'-design structure (*e.g.* **NAS-1**, Fig. 6). Some of these NAS LMWGs were compatible with mammalian cells, albeit only HeLa cancer cells were tested in early work.[80,81] Working on their NAS design strategy, Xu and co-workers later developed a hydrogel based on **NAS-2** (Fig. 6) that combined nucleobase (adenine), peptide (RGD) and saccharide (glucosamine).[82] LMWG assembly promoted murine embryonic stem cell proliferation. The authors modified the structure by removing glucosamine, exchanging aspartic acid with glutamic acid or using thymine instead of adenine to obtain three analogues, each of which formed similar gels to the unmodified LMWG. However, the modified LMWGs did not enhance stem cell growth, and neither did each individual motif if added in non-assembling form. Thus,

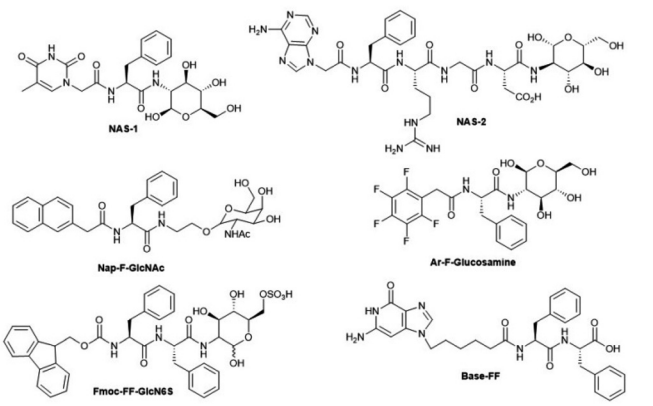

Fig. 6 Selected chemical structures of LMWGs that combine multiple bio-derived fragments in a single molecule.

each part of the LMWG is necessary for function. It was reasoned that RGD provides adhesion, while adenine and glucosamine may interact with other, undefined, cellular proteins/enzymes. The authors reflected that the structural variability of LMWGs should readily facilitate further tuning to meet specific cell requirements.

In relatively early work from 2011, Wang and co-workers modified phenylalanine with three different saccharides.[83] Gelation was tested using a simple heat-cool method and only one derivative (**Nap-F-GlcNAc**, Fig. 6) assembled into a hydrogel. Cell viability assays showed this hydrogel was compatible with fibroblasts, which adhered to the gel and proliferated well. Lin and co-workers also modified phenylalanine, in this case with a fluorinated aromatic ring and a sugar unit (glucosamine) (**Ar-F-Glucosamine**, Fig. 6). Glucosamine is a particularly easy sugar to incorporate because of its nucleophilic amine, which can be easily synthetically differentiated from the many alcohols. The surfactant-like structure formed a hydrogel at physiological pH.[84] On modifying the number of fluorine atoms, changing the amino acid to glycine, or removing glucosamine, the LMWG could no longer form gels, demonstrating the careful structural balance. This hydrogel was non-cytotoxic to hMSCs (3A6-RFP), supporting proliferation. Glucosamine can encourage chondrogenesis, and hMSCs growing on the gel expressed SOX9, typical of this type of differentiation. It was also shown that hMSCs could secrete paracrine factors, which downregulate the fibrotic genes in skin fibroblasts, suggesting this hydrogel may have potential applications in wound healing.

Pires and co-workers also combined glucosamine with a peptide, conjugating **Fmoc-FF** with glucosamine-6-sulfate to create **Fmoc-FF**-GlcN6S (Fig. 6).[85] This assembled into self-healing hydrogels with improved cytocompatibility towards human adipose-derived stem cells (hASCs) when compared to **Fmoc-FF** alone. Under basal conditions (*i.e.*, without any specific differentiation factors), hASCs overexpressed neural markers, such as GFAP, Nestin, MAP2, and βIII-tubulin, confirming differentiation into neural lineages. The authors hypothesised glycosylation is crucial for the biofunctionality by capturing and preserving essential growth factors produced endogeneously during differentiation, *e.g.*, FGF-2. To explore this, they deliberately loaded FGF-2 into the glycopeptide gel and showed the gel maintained bioactivity over 3 days, but when FGF-2 was loaded into a simple **Fmoc-FF** gel, it did not.

Recently, Das and co-workers developed nucleobases conjugated with peptides to examine the effect of amino acid hydrophobicity.[86] After gelation tests in phosphate buffer using ultrasound, only nucleobase-functionalized diphenylalanines (*e.g.* **Base-FF**, Fig. 6) formed hydrogels. This is in-line with hydrophobic phenylalanine being a privileged amino acid for gelation, and indicates the peptide plays a key role in self-assembly. The hydrogel was cytotoxic to epithelial cells at high concentrations but suitable for culturing McCoy fibroblasts at all concentrations.

2.3.4 'Synthetic' gelators. Moving beyond biologically derived building blocks, LMWGs based on synthetic scaffolds can also be used in cell growth. For example, benzene tris-carboxamide (BTA) derivatives are well-known to assemble into supramolecular polymers as a result of π–π stacking of the aromatic rings, and intermolecular hydrogen bonds between amides.[87] In 2020, Palmans, Meijer and co-workers explored BTA hydrogels as potential bioactive materials for cell growth, albeit with cancer cells.[88] The BTA derivatives were functionalised with peripheral tetraethylene glycol or mannose units to provide water solubility (**BTA-OEG$_4$** and **BTA-Man**, Fig. 7). Baker and co-workers developed hydrogels based on mono- and bis-BTA derivatives with PEG substitution.[89] Each could form hydrogels, however, when they were combined, the bis-BTA system enabled crosslinking between BTA stacks – different ratios of the building blocks tune the rheology of the gels. The hydrogels were cytocompatible with fibroblasts, and the self-healing characteristics allowed cells to be encapsulated within the 3D matrix. However, when chondrocytes (ATDC5) were cultured on the gel, up to 20% of cells were non-viable. The authors explored neuronal cells (PC12s) observing a degree of cell aggregation, followed by neurite outgrowth. The authors also achieved aggregation of hMSCs and could even fuse pre-formed hMSC spheroids in the hydrogel – a strong indication of viable hMSCs. Aggregation appeared to correlate with the dynamics of the gel – an important topic we return to in section 3.2.

Bis-ureas have been privileged scaffolds for the formation of synthetic gels since their original development in greases for use in the automotive industry.[5] They are easily synthesised *via* reaction between amines and isocyanates and self-assemble into 1D-structures as a result of complementary intermolecular hydrogen bond interactions between urea groups.[90] Modification with hydrophilic substituents enables their use in water, with Dankers, Sijbesma and co-workers making use of this design principle to modify bis-ureas with sugars, creating a hydrogel capable of supporting cell growth.[91] This also demonstrates the modification of a synthetic assembling motif with bioactive units. In this case, the selected sugars were proposed to bind to asialoglycoprotein receptors (ASGPRs) in the hepatic cells being studied. This important concept of incor-

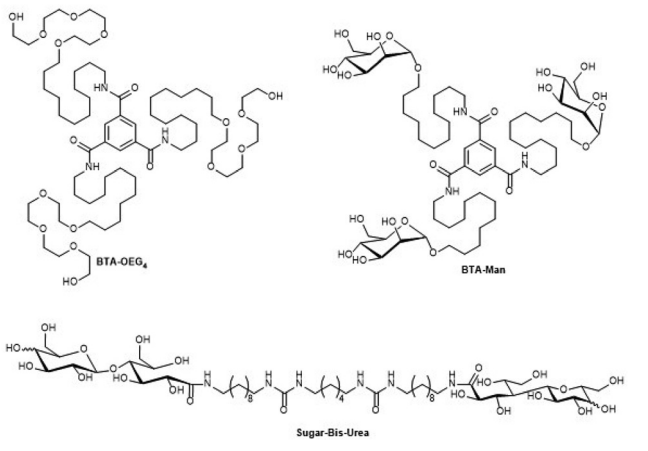

Fig. 7 Selected chemical structures of LMWGs based on synthetic scaffolds.

porating bioactive cues into an LMWG hydrogel is one we return to in section 5.2.

2.4 Multi-component LMWG hydrogel assembly

A key advantage of the LMWG approach to gel assembly is that multiple components can easily be combined *via* simple co-formulation. Understanding the self-assembly of multi-component gels is of fundamental importance in soft materials science, requiring insight into supramolecular kinetic and thermodynamic preferences.[92,93] In general, LMWGs will co-assemble if their mutual interactions are favoured, often as a result of having similar structures or being simultaneously assembled. Self-sorting of LMWGs is more likely if the structures are significantly different, with assembly relying on orthogonal non-covalent interactions, or if the LMWGs are triggered to assemble sequentially using different stimuli. As illustrated in the following sections, multi-component systems can have unique impacts on biological outcomes.

2.4.1 Co-assembly – a supramolecular strategy to diversify LMWGs. The examples in section 2.3 showed how different molecular motifs support cell growth. However, as more functionalities are incorporated into a single LMWG, this introduces synthetic complexity and cost, diminishing the advantage of LMWG hydrogels as simple, accessible materials. Furthermore, each additional functional group increases the chance self-assembly will be disrupted. An alternative approach is to harness non-covalent interactions and use co-assembly to incorporate a second component into the self-assembled nanostructure.

In Ulijn and co-workers' initial 2006 work on the use of **Fmoc-FF** for cell growth (see section 2.2), they made rudimentary use of co-assembly, mixing Fmoc-K with **Fmoc-FF** and demonstrating that the resulting gel slightly improved cell proliferation, giving the first hints of the power and simplicity of this approach.[46] In 2009, Ulijn and co-workers elegantly expanded the use of co-assembly.[94] They demonstrated that on **Fmoc-FF**, human dermal fibroblasts exhibited a rounded morphology, and to enhance growth, reasoned it was necessary to endow the scaffold with better cell adhesion. They therefore co-assembled **Fmoc-FF** with **Fmoc-RGD** at various loadings. **Fmoc-FF** drives assembly, while **Fmoc-RGD** can be incorporated into the self-assembled structures (Fig. 8a and b). The co-assembled gels were used as 3D scaffolds with anchorage-dependent human dermal fibroblast cells, which exhibited enhanced proliferation in the presence of **Fmoc-RGD**. After 3 days, the gel contracted very significantly. The authors proposed that spread cells formed a 3D-network up to day 3, which pulled the nanofibres to which they had adhered, and remodelled the extracellular fibrous matrix – a phenomenon similar to wound contraction *in vivo* (Fig. 8c and e). When performing co-assembly using Fmoc-RGE, a non-adhesive peptide analogue, these processes were less effective (Fig. 8d).

At a similar time, co-assembly was being used by Collier and co-workers to modify their larger self-assembling peptide gels.[95] They combined self assembling peptides (QQKFQFQFEQQ) that formed β-sheets with variants that

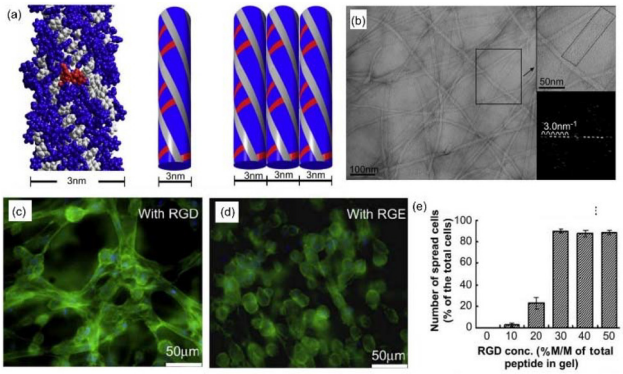

Fig. 8 (a) Co-assembly of **Fmoc-FF** (blue) and **Fmoc-RGD** (red) gives nanofibres with a diameter of 3 nm. Schematic diagram indicates self-assembly into nanostructures that display RGD ligands on the surface. (b) TEM image indicating the formation of flat ribbons comprising parallel-aligned fine fibrils (diameter 3 nm) across their width. (c and d) Cell adhesion and morphology in (c) **Fmoc-FF**/RGD and (d) **Fmoc-FF**/RGE with adult dermal fibroblasts showing spreading leading to a three-dimensional network in (c) and rounded morphologies in (d). (e) Impact of **Fmoc-RGD** loading in the co-assembled gel on cell spreading. Figure adapted from ref. 94 with permission of Elsevier, copyright 2009.

expressed RGDS or IKVAV ligands on the fibril surfaces. It was possible to tune the level of co-assembled ligand incorporation without significantly changing the physical properties of the gel. The presence of these bioactive epitopes influenced the attachment, spreading and morphology of human umbilical vein endothelial cells (HUVECs). When the RGDS-modified peptide was co-assembled, HUVEC attachment, spreading and growth were increased, whereas IKVAV had a more subtle effect on cell attachment and morphology.

In 2010, Stupp and co-workers approached cartilage regeneration *via* co-assembly using their large peptide amphiphiles (PAs).[96] They developed self-assembling PAs displaying HSNGLPL peptides that bind transforming growth factor β-1 (TGFβ-1) and co-assembled them with their standard PA. Growth factor release studies showed passive release of TGFβ-1 was slower from gels containing growth factor binding sites. *In vitro* studies indicated these materials supported hMSC survival and promoted chondrogenic differentiation. The gels were also capable of promoting regeneration of articular cartilage in a rabbit model with, or even without, the addition of exogenous growth factor.

As a recent example of co-assembly in larger peptides, Yu and co-workers combined two larger peptides.[97] These were modified with peptide sequences QHREDGS (derived from angiopoietin-1), and GRGDS (derived from osteopontin) both of which play different roles in integrin binding. Co-assembly yielded a bioactive hydrogel with outstanding stability and the ability to stimulate HUVEC cell growth, adhesion, and migration. The levels of CD31, bFGF, and VEGF in HUVECs exposed to the self-assembled functional peptide hydrogels were greater than in the control group, indicating the co-assembled gel promoted angiogenesis, with potential applications in wound healing. However, when applied to larger

peptides, co-assembly actually requires the synthesis of several large complex peptides. The power of co-assembly is more obviously realised in low-molecular-weight systems, in which function can be amplified with minimal synthetic input or cost – as originally demonstrated by Ulijn and co-workers (see above).

Das and co-workers synthesized an LMWG based on alanine functionalised with a guanine nucleobase that co-assembled with other guanosine derivatives to form gels *via* mixed G-quartet assembly.[98] McCoy fibroblasts showed good metabolic activity in 2D culture on the co-assembled hydrogels. Furthermore, the hydrogels had anti-inflammatory function and could accelerate wound closure.

Recently, we co-assembled **DBS-CONHNH$_2$** and **DBS-CH$_2$OH** (see section 2.3.2).[79] Careful thermodynamic characterisation indicated the two LMWGs formed a single combined nanostructure. They each gave the resulting co-assembled gel some of their own properties in terms of hMSC growth, with **DBS-CONHNH$_2$** directing cell morphology and **DBS-CH$_2$OH** controlling cell penetration into the gel.

At the interface between LMWG hydrogels and polymer gels, Dankers and co-workers formed gels based on the co-assembly of **UPy** derivatives (see section 2.3.1). They combined **UPy** functionalised with cyclic-RGD and a second self-assembling **UPy** derivative to form solution-phase supramolecular polymers.[99] The addition of a bis-functionalised **UPy** derivative with a polymeric linker triggered gel formation. Based on the ratios of the component parts, it was possible to tune the effective ligand density of cyclic-RGD. The gels were used to culture MDCK mammalian epithelial cells. In 2D culture, a higher effective ligand concentration overruled the influence of stiffness in dictating cell adhesion and polarity – *i.e.*, multivalency wins. However, in 3D culture, only in gels with physiological stiffness was the effective ligand concentration able to regulate the polarity and self-organization of cellular structures – *i.e.*, multivalency and mechanical properties must collaborate. The importance of network mechanics on cell growth in gels is discussed in more detail in section 3.1.

In addition to the co-assembly of different LMWGs, it is also possible to use co-assembly to modify a pre-assembled LMWG network. Banerjee and co-workers reported a histidine-containing peptide hydrogel, the macroscopic properties of which were improved by adding dicarboxylic acids (*e.g.* oxalic acid, succinic acid), which interact with the basic histidine unit.[100] Incorporating succinic acid into the peptide hydrogel induced the greatest enhancement of mechanical and thermal properties, and this hydrogel was successfully used to culture mouse NIH-3T3 fibroblasts *in vitro* for 2 days, with cell penetration showing some dependence on gel stiffness.

Co-assembly of several interacting building blocks into a single integrated network by simple co-formulation cannot so easily be achieved with polymer hydrogels and constitutes a significant advantage of LMWG hydrogels. Additionally, the loading-level of co-assembled supramolecular systems can be easily varied, potentially changing the output, meaning such gels are synthetically simple, easily tuned, bioactive materials. In later sections, further examples use co-assembly as a stepping-stone to create gels that direct cell growth outcomes in unique and interesting ways.

2.4.2 Self-sorting – a supramolecular strategy to generate dual-network LMWG hydrogels. LMWG self-sorting typically gives rise to two independent gel networks interpenetrated with one another. In polymer science there is considerable interest in dual-network hydrogels as biomaterials,[101] but although self-sorted LMWG hydrogels have been investigated at a fundamental level,[102] they have been less widely explored in terms of tissue engineering potential.

In 2019, Mata and co-workers reported a self-sorted hydrogel that combined a peptide amphiphile with sorbitol-derived DBS-CO$_2$H, previously reported by our group (Fig. 9a).[103] During self-assembly, DBS-CO$_2$H initially acted as an additive adsorbed on the surface of the PA nanofibers through multiple hydrogen-bonds. The adsorbed DBS-CO$_2$H in close proximity then interacted with each other and self-assembled into their own nanofibres, thus facilitating interactions between the PA nanostructures (Fig. 9b). Compared to the individual components, the resulting self-sorted multi-component hydrogel had improved stiffness (from DBS-CO$_2$H), self-healing character (endowed by the PA), and stability to enzymatic degradation (provided by DBS-CO$_2$H). Importantly, the self-sorted two-com-

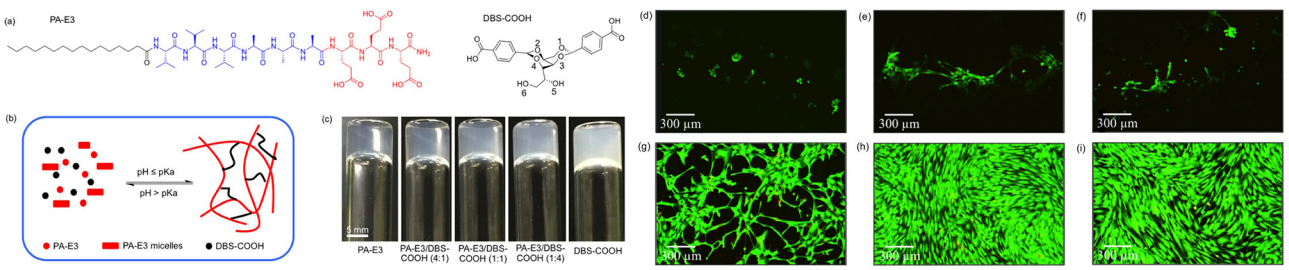

Fig. 9 (a) Peptide amphiphile (**PA-E3**) and LMWG **DBS-COOH**. (b) Schematic of self-assembly in which **DBS-COOH** fibres are nucleated on **PA-E3** nanofibres. (c) Photographic images of self-assembled hydrogel samples formed by different combinations of the LMWGs. (d–i) Laser scanning confocal microscopy images of human-adipose-derived stem cells seeded on hydrogels of (d) **PA-E3**, (e) **PA-E3/DBS-COOH** (4 : 1), (f) **PA-E3/DBS-COOH** (1 : 1), (g) **PA-E3/DBS-COOH** (1 : 4), (h) **DBS-COOH**, and (i) cells plated on tissue culture plastic for 4 days. Figure adapted from ref. 103 with permission of the American Chemical Society, copyright 2019.

ponent gels (Fig. 9c) were compatible with human adipose-derived stem cells, which would only grow if sufficient DBS-CO_2H was present (Fig. 9d–i). This demonstrates how tuning components in self-sorting systems can yield dual-network hydrogels in which the different networks act synergistically, and the overall gel performs as more than the sum of its individual parts.

3 Impact of network properties on cell growth

3.1 Mechanical control of cell growth outcomes

One of the most intriguing aspects of stem cells is their ability to respond to the environment in which they are placed. Indeed, this is one of the ways living systems use the extracellular matrix to direct stem cells to take on specific roles during healing and growth processes. For example, a stiffer extracellular matrix encourages mesenchymal stem cells to regenerate bone, whereas softer matrices encourage cartilage or fat formation.[104] This response of stem cells to stiffness has been used for some time to direct the design of polymer hydrogels that control stem cell differentiation.[105]

In terms of LMWG hydrogels, the first hints about the impact of gel matrix stiffness on the fate of stem cells emerged in 2015, in work from Barthélémy and co-workers.[66] As noted in section 2.3.1, their bola-amphiphilic **GNBA**-based gel was significantly stiffer than their earlier **GNF** system. When hMSCs were encapsulated in the stiffer **GNBA** gel, they grew with spindle-shaped morphology. On the contrary, in the softer **GNF** hydrogel, rounded cells were detected. The authors argued these differences were a result of the mechanical differences, with the stiffer gel promoting cell adhesion and spreading.

In 2016, the first examples were published in which an LMWG hydrogel explicitly controlled stem cell differentiation because of its rheological properties. Dalby, Ulijn and co-workers co-assembled **Fmoc-FF** with Fmoc-S (Fig. 10a).[106] The LMWG loadings could be altered to regulate the mechanical properties and hence direct the differentiation of perivascular stem cells (Fig. 10b). This reinforces the benefits of co-assembly as a powerful supramolecular strategy for directing biological outcomes (see section 2.4.1). On soft (1 kPa), stiff (13 kPa), and rigid (32 kPa) gels (Fig. 10c), neuronal, chondrogenic, and osteogenic differentiation, respectively, were observed. Stem cell differentiation led to metabolite depletion, and in this case, the researchers also used the different gels to understand the impact of metabolites on differentiation pathways. Adding the newly uncovered metabolites back into cell growth assays further facilitated differentiation (Fig. 10d). This demonstrates how LMWG hydrogels, in addition to being interesting biomaterials, can be used as tools to understand and manipulate stem cells.

Also in 2016, Gao, He and co-workers synthesised a peptide LMWG modified with a phenylboronic acid.[107] The resulting gels had tunable stiffness depending on loading and solvent composition (PEG200:H_2O). MSCs were seeded on gel surfaces, which exhibited good proliferation, with confocal microscopy demonstrating migration of cells from surface to bulk. Cell morphology was different in gels with different stiffnesses. Furthermore, ALP expression from the stiffer gels was greater than in the softest gels, indicative of osteogenesis. This was supported by the greater secretion of ColI and OCN from cells grown on the stiffer gels, while, cells grown on the softer gels exhibited higher levels of Sox2 and ColII, indicative of chondrogenesis. The researchers found the critical modulus to determine whether MSCs differentiated into chondrocytes or osteoblasts was 10–20 kPa. Using PEG200 as a co-solvent is a drawback, but there was clear evidence of rheological control over cell growth outcomes. In later work, the same researchers demonstrated that altering the length of the LMWG alkyl chain could also tune rheology and hence impact on cell growth.[108] Once again, MSCs tended to differentiate into osteoblasts in stiff gels (20–40 kPa) and chondrocytes in soft gels (1–10 kPa).

Lin and co-workers co-assembled **Fmoc-FF** with five different bioactive peptides that incorporated the HAV sequence, and were hence mimetics of *N*-cadherin, a calcium-dependent adhesion molecule.[109] The resulting gels had variable stiffnesses and were cytocompatible with hMSCs (3A6). The multi-component gel with the highest stiffness (*ca.* 20 kPa) promoted chondrogenic differentiation, while cells cultured in softer multi-component gels showed lower levels of chondrogenesis. This suggested the stiffer gel is a promising material for cartilage regeneration, demonstrating the importance of optimising both gel rheology and peptide sequence.

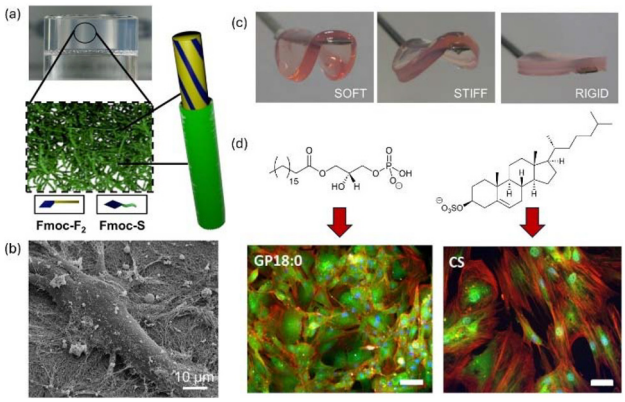

Fig. 10 (a) **Fmoc-FF** and Fmoc-S co-assemble into nanofibres that form a self-supporting hydrogel. (b) SEM image of a single mesenchymal stem cell attached to 50 : 50 **Fmoc-FF**/Fmoc-S nanofibres. (c) Photographs of gel samples indicating the tunability of the mechanical properties of 50 : 50 **Fmoc-FF**/Fmoc-S (dependent on total loading) from soft to stiff to rigid. (d) Compounds **GP18:0** (left) and **CS** (right) were identified as being depleted when MSCs were grown on stiff and rigid hydrogels, giving rise to chondrogenesis and osteogenesis respectively. When MSCs were grown in the presence of these bioactives, (left) significant SOX-9 expression was observed in the presence of **GP18:0** and (right) osteopontin staining indicated a significant increase in expression in the presence of **CS**. Figure adapted from ref. 106 with permission of Cell Press, copyright 2016.

Interestingly, the gel stiffness is similar to that reported by Gao and He for osteogenesis, yet here, chondrogenesis is observed. However, the cell lines are different and may respond differently to mechanical cues. Furthermore, the LMWG structures are also different, which can induce different levels of cell adhesion, which couple with mechanical factors to lead to different cell growth outcomes. Therefore, although general principles associated with gel stiffness can be applied, these should not be taken as quantitatively literal – careful experimental study of varied LMWG hydrogels with specific cells of interest are vital.

It is therefore important to recognise that gel network mechanics do not act alone in controlling stem cell growth, but intersect with gel dynamics, adhesion ligands, functional group modifications and cell types in terms of mediating the way stem cells interact with gel networks, controlling cell proliferation and differentiation. Later sections of this review explore these themes in more detail.

Working with fibroblasts, Tirrell and co-workers designed pH-responsive histidine- and serine-containing peptide amphiphiles with spacers based on either glycine or ethylene oxide.[110] The choice of spacer impacted on gel stiffness, with glycine resulting in a stiffer gel as a result of hydrogen bonding, while ethylene oxide, which disrupts H-bonding, gave a softer gel. The stiffer gel was compatible with NIH 3T3 fibroblasts, with spindle-like cells resulting. However, the softer gel was not tested, so it is not completely clear whether mechanical tuning played an essential role in performance in this case.

In 2019, Stupp and co-workers reported a hydrogel based on a larger peptide with tuneable mechanical stiffness, allowing for very precise control over stiffness.[111] The system combined a negatively charged PA with a positively charged oligo-L-lysine. The hydrogel mechanical properties were incrementally increased (*ca.* 10 Pa at a time) by iteratively placing lysine residues in the oligo-lysine. Conjugating a bioactive peptide on the C-terminus did not significantly impact gel stiffness. The gel was used to culture neural stem cells and supported neuronal differentiation, with the viability of neurons being better on softer gels, and a change in storage modulus of just 70 Pa significantly affecting cellular outcomes, including cell survival, tyrosine hydroxylase expression, and neurite growth. The authors suggested potential applications for transplantation therapy in Parkinson's disease. As such, surprisingly subtle tuning of structure and gel properties may optimise performance in biological systems. Clearly, biology has evolved to control such processes with a high degree of precision – multicomponent supramolecular approaches offer a way of approaching this level of control.

Dankers and co-workers recently demonstrated that bulk gel stiffness may not be enough to fully understand cell behaviour.[99] After all, cells interact with gel fibres on the microscale level, not at the level of the bulk material. Using nanoindentation, they demonstrated that a series of gels with increasing LMWG loadings had increasing bulk stiffnesses (0.1–8 kPa), but surprisingly all had similar local stiffnesses (*ca.* 10 kPa). Interestingly, in interpenetrated polymer gels, cells have been shown to behave depending on the stiffness of the network they are attached to, rather than the overall bulk stiffness.[112] Clearly future work on supramolecular systems needs to distinguish between local mechanical effects experienced by individual cells, and overall bulk rheology, which impacts on the cell culture as a whole. The tunability of LMWG hydrogel systems across multiple length scales is actually a key potential advantage in terms of cell culture, as will be illustrated in future sections.

3.2 Impact of gel dynamics on cell growth

Beyond the well-established impact of hydrogel mechanical properties on cell growth, it has recently become clear that the dynamics of a substrate on which cells are growing can also play a key role. Such effects have been established for extracellular matrix and polymeric materials.[113] Given LMWG hydrogels are, by their very nature, highly dynamic materials across multiple length scales, there is a unique opportunity to design scaffolds where the dynamics instruct and direct growing cells.

In a key paper from 2021, working at the interface between LMWG and polymer gels, Dankers and co-workers demonstrated that larger supramolecular systems incorporating interactive **UPy** units (Fig. 5) could form gels with different dynamics.[70] Combining **UPy-PEG-UPy** with **UPy** in different ratios created hydrogels with different dynamics. Co-assembly with a cRGD-modified monomer allowed incorporation of adhesion points into the gel network. If the gel was too dynamic, cells would not show effective adhesion, irrespective of the presence of RGD. Careful study indicated that this effect arises from the high binding/unbinding rate of the UPy-cRGD additives on the molecular scale within the supramolecular fibres, preventing effective engagement of the "molecular clutches" required to drive mechanotransduction.

Dankers and co-workers went on to explore the molecular-scale dynamics of **UPy** and BTA based gels, finding they were also translated into the bulk dynamics of the gel networks (Fig. 11).[114] **UPy**-based gels exhibited slow stress relaxation ($\tau_{1/2} \sim 1000$s) while BTA-derived gels had fast stress relaxation ($\tau_{1/2} \sim 50$s). When growing cells on these gels, they responded to these dynamics, with cell spreading being more likely on gels with slow relaxation dynamics, whereas on more dynamic gels, cells tended to remain rounded as the fast relaxation prevents the build-up of cellular traction required for spreading. Different types of cells responded in different ways. Epithelial cells responded to gel dynamics irrespective of stiffness, whereas fibroblasts only responded to gel dynamics on softer gels (*ca.* 100–200 Pa) while at greater stiffnesses (*ca.* 1000 Pa), the stiffness overruled dynamics. These results demonstrate an interplay between dynamics and stiffness in terms of controlling cell growth, with dynamics being particularly important in softer gels. The results also emphasise the importance of carefully understanding specific cell-types on LMWG hydrogels. In this example, stem cells were not studied.

Working with hMSCs, we recently explored the behaviour of **DBS-CH$_2$OH** and compared its behaviour against well-estab-

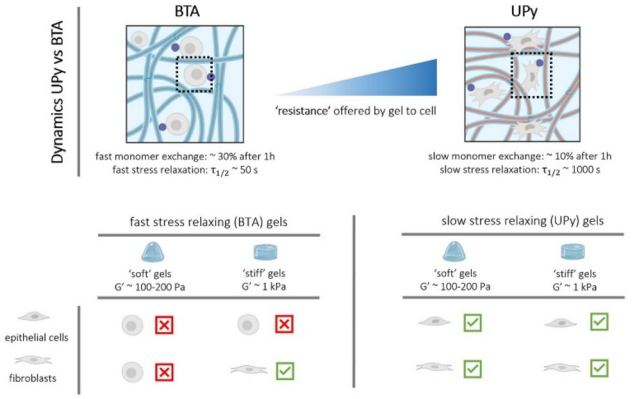

Fig. 11 Cartoon showing differences in molecular dynamics (monomer exchange) and bulk dynamics (stress relaxation) between BTA and **UPy** supramolecular fibres and hydrogels as reported by Dankers and co-workers. BTA exhibits faster molecular and bulk dynamics, which prevent cell spreading on soft gels. However, on stiff gels, the stiffness can, for fibroblasts, overrule the influence of gel dynamics, resulting in cell spreading. **UPy** has slower dynamics enabling cell spreading in all cases, irrespective of gel stiffness. Figure reproduced from ref. 114 with permission of the American Chemical Society, copyright 2023.

lished **DBS-CONHNH$_2$** (see section 2.3.2).[79] The softer **DBS-CONHNH$_2$** gel (G' = 610 Pa) gave rounded hMSCs, while the stiffer **DBS-CH$_2$OH** gel (G' = 3430 Pa) induced a spread hMSC morphology (Fig. 12). Initially, we assigned this to gel stiffness alone. However, the co-assembled gel combining both **DBS-CONHNH$_2$** and **DBS-CH$_2$OH** had high stiffness (>5000 Pa) but surprisingly caused hMSCs to proliferate with a

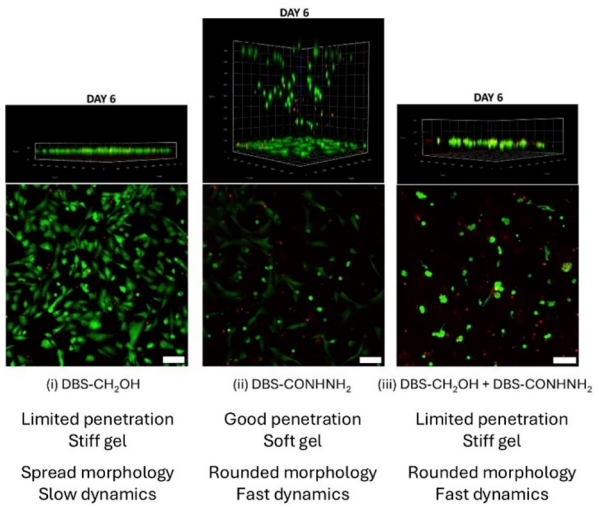

Fig. 12 3D confocal microscopy images (top) and z-axis maximum projection images (below) of Y201 hMSCs growth on (i) **DBS-CH$_2$OH** (0.3% wt/vol), (ii) **DBS-CONHNH$_2$** (0.3% wt/vol) and (iii) **DBS-CH$_2$OH**/**DBS-CONHNH$_2$** (0.3/0.3% wt/vol) showing live stain (Calcein AM, green) and dead stain (PI, red) at day 6. Scale bar of 100 μm. Key features of cell penetration and morphology are highlighted and linked to macroscopic properties of the different gels. Figure adapted from ref. 79 with permission of Wiley-VCH, copyright 2026.

rounded morphology. It therefore appeared that gel stiffness controlled the penetration of hMSCs into the gels but could not fully explain the observed hMSC morphologies. Stress relaxation experiments indicated little difference in gel dynamics at the network level, which were very fast in all cases. However, using NMR to probe molecular-scale mobility and determine gel thermodynamics, we found that **DBS-CH$_2$OH** had a much higher enthalpy and entropy of dissociation than the other gels, and individual LMWG molecules were much less soluble/mobile. In contrast, gels incorporating **DBS-CONHNH$_2$**, including the gel that co-assembled **DBS-CH$_2$OH** and **DBS-CONHNH$_2$**, had greater molecular-scale LMWG dynamics. We concluded the molecular-scale dynamics of the gel were likely playing a role in mediating hMSC growth outcomes, with low dynamics helping support the spread hMSC morphology on **DBS-CH$_2$OH**. It is also possible that the different functional groups on the two LMWGs play a role in mediating cell growth morphology (see section 3.3).

Stupp and co-workers have been interested in dynamics in gel fibres that incorporate bioactive cues.[115] They synthesised relatively large PAs with two peptide sequences – one that reduces glial scarring and another that promotes blood vessel formation (Fig. 13a). By mutating an amino acid in the peptide domain outside of the signalling region, they induced enhanced supramolecular motion of the molecular building blocks within the fibrils (Fig. 13b). Using human neural progenitor cells (hNPCs) derived from human embryonic stem cells, they found that the self-assembled fibres with enhanced dynamics induced higher concentrations of the β1-integrin transmembrane receptor and the downstream effectors (integrin-linked kinase and phospho-focal adhesion kinase). The hNPCs also exhibited greater up-regulation of the neuronal form of β-tubulin (Fig. 13c). On adding $CaCl_2$ (5 mM), which suppressed the supramolecular motion, the desired activation of the β1-integrin pathway was also inhibited. These dynamic systems were applied in co-assemblies with FGF peptide amphiphiles in a mouse model of paralysing human spinal cord injury and there was greater functional recovery when using the more dynamic PA co-assemblies (Fig. 13d). The authors suggested that a dynamic supramolecular scaffold could be more effective at signalling receptors in cell membranes undergoing rapid shape fluctuations, or that there are more favourable interactions of dynamic scaffolds within the complex ECM environment. They noted the prevalence of intrinsically disordered proteins in biology and hypothesised that dynamic supramolecular systems may be more powerful than previously realised. A similar approach was also applied to HIPSC-derived motor and cortical neurons, showing that highly mobile PA scaffolds enhanced β1-integrin pathway activation, reduced aggregation, increased arborization, and matured electrophysiological activity of neurons.[116]

Working with polymer hydrogels, a variety of other effects of dynamics on cell growth have also been observed.[117–119] For example, more dynamic gels have been shown to encourage cell spreading or promote tissue growth, with it being argued that cells are able to better remodel their surrounding matrix.

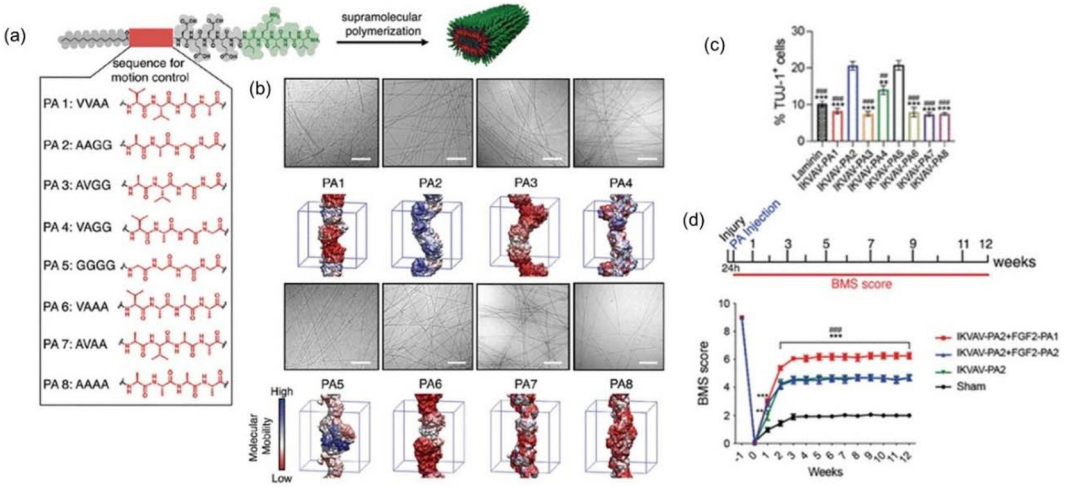

Fig. 13 (a) Specific chemical structures of IKVAV PA molecules used and molecular graphics representation of a supramolecular nanofiber displaying the IKVAV bioactive signal. (b) Cryo-TEM micrographs of IKVAV PAs in the library (scale bars 200 nm) and their corresponding color-coded representations of root mean square fluctuation (RMSF) values for single IKVAV PA filaments derived from molecular dynamics simulation with red representing low mobility and blue representing high mobility. (c) Bar graph of the percentage of TUJ-1^{+} neuronal cells treated with the various IKVAV PAs. Error bars correspond to three independent differentiations. (d) Experimental timeline of *in vivo* experiments (top) and BMS for locomotion (bottom). Error bars correspond to 38 animals per group. Figure adapted from ref. 115 with permission of Science, copyright 2021.

Indeed, in Stupp's work described above on integrin upregulation, there was a preference for more dynamic supramolecular assemblies. However, when Dankers and ourselves considered cell adhesion and traction, less dynamic assemblies appeared more effective. This demonstrates how supramolecular dynamics may have to be optimised in different ways for different biological outcomes. In comparison to polymeric scaffolds, work on the dynamics of LMWG hydrogels remains at a nascent stage and there is great scope for understanding and optimising dynamic processes, especially given the inherent dynamics of supramolecular systems are one of their key advantages. Furthermore, the multi-scale nature of LMWG hydrogels – from molecular-scale through to nano-, micro- and macro-scale means dynamics can potentially be controlled on multiple different levels that may interact with cells, which are also multiscale systems, in very different ways.

3.3 Chemical microenvironment

In addition to the mechanical properties and dynamic behaviour of the self-assembled network, it is recognised that the chemical microenvironment of the gel network also plays a key role in influencing stem cell growth. The importance of specific adhesion ligands, such as RGD and IKVAV has already been noted in other sections. However, beyond such binding epitopes, general chemical functionality can also play a role.

Seminal work from Anseth and co-workers in 2008 demonstrated this principle in polymer hydrogels, showing that hMSCs differentiated down adipogenic or osteogenic pathways depending on whether the PEG polymer gel was functionalised with *t*-butyl or phosphate groups.[120] They suggested that the functional groups can cause cell–matrix interactions that induce differentiation leading to the production of tissue specific matrix molecules or that the chemical environment may interact with and nucleate particular cell-secreted molecules, hence directing differentiation.

Building on these insights, in 2009 Ulijn and co-workers incorporated a range of different chemical functionalities into a self-assembled **Fmoc-FF** LMWG hydrogel by co-assembly with Fmoc-K, Fmoc-D and Fmoc-S.[121] All compositions gave rise to self-assembled nanofibrillar gels with elastic moduli varying from 502 Pa (**Fmoc-FF**/Fmoc-D) to 21200 Pa (**Fmoc-FF**). Different compositions supported different cell types, with **Fmoc-FF**/Fmoc-S being the only gel that supported all cells investigated, and also retained cell morphology in 3D culture of bovine chondrocytes. The authors assigned these differences to the chemical functionality being programmed into the gel scaffold *via* co-assembly and suggested that a tunable chemical microenvironment can play a key role in supporting cell growth. This early work stimulated significant further study of functional group modification across a wide range of peptide LMWGs, for example using different peptide sequences (see section 2.2).

Using small peptide amphiphiles, Guler, Tekinay and co-workers created a series of PAs modified with the different functional group components of glycosaminoglycans (*i.e.* glucose, carboxylate, sulfonate).[122] The ratio of functional groups on the co-assembled nanofibres influenced the differentiation of rat mesenchymal stem cells, with a higher sulfonate-to-glucose ratio being inducing adipogenesis and a higher carboxylate-to-glucose ratio being associated with osteochondrogenic differentiation. The authors concluded that distinct biomimetic signals were presented to the cells on the synthetic ECM mimetic as a result of the functional groups.

It is increasingly clear that a wide range of factors influence cell growth outcomes,[123,124] including mechanical properties,

dynamic behaviour, adhesion ligands, and chemical microenvironment. In many cases, changing functional groups in an LMWG induces other changes in mechanical properties and gel dynamics. In future work, it will be increasingly important to carefully untangle the different factors to determine which are operational in any specific gel-cell system.

4 Impact of LMWG chirality on cell growth

It is well-known that chirality can direct gel self-assembly in a variety of ways.[125,126] In many self-assembled gels, molecular-scale chirality is translated into the nanoscale morphologies that underpin the gel. Given living systems are themselves inherently chiral, the chirality of the LMWG and the nanoscale assembled scaffold can potentially have significant influences on cell growth.

As discussed in section 2.2, peptides constructed from L-amino acids are sensitive to proteolysis – one way of avoiding this is to construct peptidic gels using D-amino acids, which are typically not natural substrates for proteolytic enzymes.[127] An early example using D-peptides to produce gels for cell growth was provided by Luo and co-workers who, inspired by the large self-assembling peptides first reported by Zhang and co-workers, developed peptide 16-mers based on D-amino acid building blocks.[128] The resulting D-peptide hydrogels were used for 3D culture of carcinoma cells and demonstrated similar levels of cell proliferation and apoptosis to an L-peptide analogue. They did not determine the stability of the gel to protease enzymes, and the work needed extending to stem cells, but this was a key step towards cell culture in D-peptide hydrogels.

Working with shorter peptide hydrogels, the *in vivo* biostability, biodistribution, and toxicity of supramolecular nanofibers formed by Nap-GFFYGRGD and Nap-G^{D}F^{D}F^{D}YGRGD have been studied. The D-peptide had better *in vitro* and *in vivo* biostabilities than the L-peptide analogue – the D-fibres were stable in plasma for 24 h while half of the L-fibres were digested in just 6 h. Maruyama and co-workers compared a D-peptide pentamer with an L-peptide analogue and showed that the D-version was completely resistant to a protease enzyme (chymotrypsin) over a 7-day period.[129] Importantly, this gel was non-toxic to embryoid bodies (EBs) derived from HIPSCs.

Beyond the stability of the gel in the biological milieu, chirality can also potentially influence the growing cells themselves. A number of studies have explored the behaviour of cells on LMWG hydrogels with different chiralities.

In 2014, Marchesan and co-workers explored the chirality of individual amino acids within a tripeptide gelator, understanding the role of chirality in directing self-assembly and the potential of heterochiral systems in cell growth.[130] The two enantiomeric LMWGs ^{D}Phe-Phe-Val and Phe-^{D}Phe-^{D}Val equally supported high viability and proliferation of mammalian fibroblast cells *in vitro*, while in solution they did not elicit a cytotoxic response. Despite one peptide having unnatural beta-sheet chirality as seen by circular dichroism spectroscopy, cells still penetrated and spread in this biomaterial over time, confirming that biomaterials for cell growth do not require a 'natural' chirality.

Driving this field forwards, Feng and co-workers have explored chirality across a number of elegant studies. They initially developed a chiral gelator based on two L (or D) phenylalanine units terminated with diethylene glycol. In 2014, working with HUVECs and fibroblasts, they observed these cells appeared to thrive in one enantiomeric form of the gel, but not the other,[131] with the L-form increasing adhesion and proliferation compared with the D-enantiomer. The authors proposed this was a result of the chirality expressed at the level of the nanofibres, suggesting differences in performance were due to binding between chiral nanofibers and fibronectin, with the stereospecificity of this interaction being demonstrated through *in vitro* binding assays.

Later studies went on to explore the interplay between self-assembled nanoscale chirality and molecular-level chirality on the growth of mouse embryonic fibroblast NIH 3T3 cells.[132,133] New LMWGs based on L-phenylalanine were synthesised, in which the spacer switched the helicity of the assembled nanostructure from left- to right-handed depending on whether it had an odd or even number of carbon atoms (Fig. 14a). Hydrogels based on L-phenylalanine showed a small but significant increase in cell adhesion on left-handed nanofibers, with a weak positive influence on cells from right-handed nanofibers (Fig. 14b). Conversely, hydrogels based on D-phenylalanine showed a weak positive influence of left-handed nanofibers and a negative influence of right-handed nanofibers. These results indicate that the molecular-scale

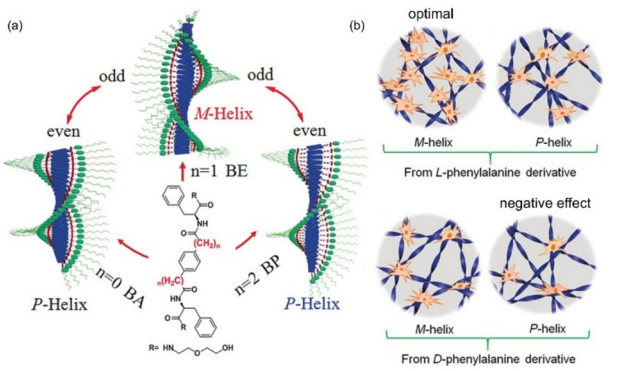

Fig. 14 (a) Chemical structure of LMWGs explored by Feng and co-workers illustrating the helical chirality inversion tuned by the variable number of methylene units. (b) Schematic illustrating (top left) the positive effect on cell adhesion on left-handed nanofibers (M-helix) derived from L-phenylalanine derivative, (top right and bottom left) the weak effect on cell adhesion on right-handed nanofibers derived from L-phenylalanine derivative and left-handed nanofibers derived from D-phenylalanine derivative, and (bottom right) the negative effect on cell adhesion of right-handed nanofibers derived from D-phenylalanine derivative. Figure adapted from ref. 132 with permission of Wiley-VCH, copyright 2018.

chirality of L-phenylalanine gives better outcomes than the D-enantiomer, but also that the nanostructures should be left-handed to optimise outcomes. This suggests chirality can operate at two wholly different length-scales in terms of mediating interactions with cells, causing subtle effects.

Feng and co-workers also used this system with human dental pulp stem cells, which exhibited greater spreading and more effective differentiation into osteoblasts on left-handed nanofibers formed by L-LMWG than the right-handed nanofibres formed by the D-LMWG.[134] Furthermore, the left-handed L-LMWG nanofibres were more effective than less-ordered planar assemblies based on the same LMWG, demonstrating it is not just the molecule that promotes cell adhesion and osteogenesis, but the specific organisation of the chiral assembly. Greater protein adsorption was demonstrated on the left-handed chiral nanofibres, and it was suggested that the stereospecificity of such interactions may provide a mechanism for the effects on stem cell growth. In later work,[135] however, it was reported that human dental pulp cells were viable in both gels, but that the L-LMWG significantly promoted adhesion of hDPSCs, while the D-analogue enhanced osteogenic differentiation by facilitating calcium entry into cells, activating the MAPK pathway. Clearly cells are complex chiral systems, and enantiomeric self-assembling systems may interact with different cells in different ways. Nonetheless, it is evident that further work is needed to fully elucidate in a predictive way, the interface between different cell types, different growth processes, and chiral self-assembling systems.

Working with MSCs, Feng and co-workers very recently showed supramolecular chirality was more important than molecular-scale chirality in terms of directing osteogenesis.[136] The authors concluded that modulation of the aromatic side chains was a key factor controlling helical bias in LMWG hydrogels, enabling the design of biomaterials with tailored chiral properties to direct stem cell fate and enhance bone tissue regeneration.

Feng and co-workers have also combined two different fragments with L-chirality, resulting in a chiral system capable of supramolecular self-sorting (see section 2.4.2), with two different fibre types being imaged by SEM.[137] This self-sorting gel was better able to promote cell proliferation, chondrogenic differentiation, and cartilage regeneration than the individual chiral hydrogels. It was suggested this results from the higher porosity and surface area, enhancing fibronectin adsorption. *In vivo* studies by injection of the gel into mice showed that the self-sorted gel regenerated subchondral bone structures found beneath the joint cartilage, with better performance than the individual LMWGs.

In recent work with this class of LMWG, Liu and co-workers coupled chirality and mechanical properties in a hydrogel.[138] By engineering the spacer chain between chiral units, they tuned the supramolecular handedness, while simultaneously modifying elastic modulus over more than an order of magnitude. Although not reporting cell growth outcomes, it seems likely that given the way multiple parameters can control the cellular microenvironment, multi-tunable systems such as this will have considerable future power.

Wang and co-workers generated hydrogels based on diastereomeric peptides containing either D- or L-phenylalanine alongside other L-amino acids.[139] The system with D-Phe chirality was self-assembled to form thixotropic nanostructured hydrogels, but the version with L-Phe chirality failed to form gels. The D-Phe-based hydrogel was used for 3D culture of mesenchymal stem cells – the cells aggregated, forming spheroids. *In vivo* experiments demonstrated that these spheroids could be applied to heal diabetic wounds, as they motivate angiogenesis and skin regeneration.

It is evident chirality plays a key role in meditating gel formation, but also in controlling the interaction between self-assembled gel nanofibres and cells. Differences between molecular-scale and supramolecular chirality again emphasise the importance of considering self-assembled gels across multiple different length-scales. As noted above, the unique multi-scale behaviour of self-assembled gels is of particular importance because cells also span multiple length scales. This stretches the understanding of supramolecular systems beyond well-established molecule–molecule interactions, emphasising the importance of considering assembly–assembly interactions at nano- and micro-scale.

5 Co-formulation to extend hydrogel scope

5.1 Combining LMWG hydrogels with other materials

In addition to combining different LMWGs *via* co-assembly or self-sorting (section 2.4), it is also possible to incorporate other nanoscale components into an LMWG hydrogel. This can significantly impact on materials properties and cell growth potential and is an easy co-formulation approach to extending the scope of LMWG hydrogels. Combining a polymer gel (PG) with an LMWG hydrogel to create a 'hybrid hydrogel' can enhance mechanical performance.[140] There are many polymeric/nanoscale components that could be combined with LMWGs to create hybrid hydrogels – this section presents selected illustrative examples relevant to cell growth.

Adler-Abramovich and co-workers used co-assembly to combine **Fmoc-FF** with **Fmoc-R** (Fig. 15a),[141] then employed the strong binding affinity of the cationic arginine group in **Fmoc-R** for polymeric anionic hydroxyapatite (HAP), which was also incorporated into the system. This created a hybrid hydrogel (Fig. 15b) and reinforced the gel, with very high stiffness being achieved (G' = 29000 Pa). Mouse 3T3 fibroblasts were grown on these gels. **Fmoc-FF** alone led to rounded cells and caused some dead cells (Fig. 15c), in the presence of co-assembled **Fmoc-R**, cells remained rounded, but once HAP was present, adherent spread cells with good viability were observed (Fig. 15d and e). It is known that HAP can promote osteogenesis, and integrating this component into gels *via* interaction with **Fmoc-R** is an interesting strategy to endow a gels with this function.

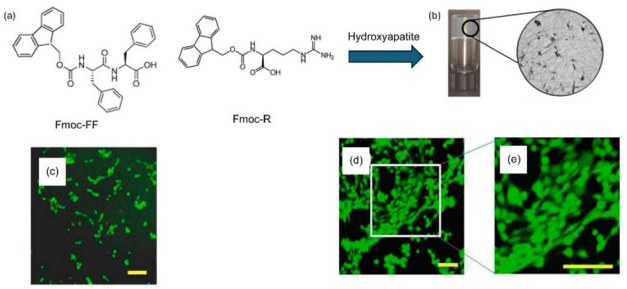

Fig. 15 (a) Molecular structure of the two building blocks **Fmoc-FF** and **Fmoc-R**. (b) Photograph of gel in upturned vial formed by FmocFF : FmocR 3 : 1-HAP and TEM image (scale bar, 1 μm). (c and d) Live–dead staining of 3T3 fibroblast cultures after 8 h treatment with FmocFF (c) and FmocFF : FmocR 3 : 1-HAP (d), including magnified inset. Green staining indicates live cells; red staining indicates dead cells. Scale bar: 500 μm. Figure adapted from ref. 141 with permission of the American Chemical Society, copyright 2017.

Cienfuegos and co-workers also co-assembled **Fmoc-FF**, this time with **Fmoc-RGD**, and incorporated the biopolymer fibrin.[142] In this case, the LMWGs enhance the mechanical properties of the otherwise weak fibrin, while the fibrin introduces biological activity. The hybrid hydrogel was cytocompatible with primary human skin fibroblasts in 2D cell culture and could degrade. At increasing loadings of **Fmoc-FF**, cell viability and proliferation were severely compromised, but as expected, **Fmoc-RGD** improved cell growth. It was therefore important to optimise the ratio of all three components. Subcutaneous injection suggested these materials were non-toxic *in vivo*, and such gels may have use in wound healing.

Chassande and co-workers combined their nucleotide-based LMWG with collagen, a naturally occurring cell-supportive biomaterial.[143] There was an interaction between the two different types of fibre. The LMWG prevented the shrinkage of collagen and limited cell diffusion out of the gel. Conversely, the presence of collagen improved cell adhesion and proliferation. The hybrid hydrogel was well-suited for long-term culture and promoted osteogenesis even in the absence of specific osteogenic cues. Cells embedded in the composite gel and injected subcutaneously in immunodeficient mice differentiated into osteoblasts and produced lamellar osteoid tissue, indicating *in vivo* potential in bone tissue engineering. This clearly shows the benefits of tuning LMWG performance by adding appropriate biopolymers (and in turn enhancing the performance of those biopolymers).

Azevedo and Radvar formed hybrid hydrogels by combining a positively charged peptide amphiphile (PA) with poly(sodium 4-styrenesulfonate) (PSS), a negatively charged synthetic polymer.[144] The concentrations were varied to control the mechanical properties. In hybrid co-formulated materials, this simple approach enables iterative tuning of the gel into the right window for performance. The PA/PSS hybrid hydrogels were loaded with proteins, including negatively charged bovine serum albumin (BSA) or positively charged lysozyme and controlled release was studied. It was suggested that PA/PSS gels may be useful for delivery of (*e.g.*) growth factors over extended time periods, which may impact on cell growth outcomes (see section 5.2 for examples of this approach). Furthermore, the anionic PSS induced some mineralisation of calcium salts – a desirable feature in materials for osteogenesis. The gels were non-toxic towards encapsulated hMSCs and the combination of multiple cues in the one system makes them promising materials for 3D cell differentiation.

In elegant work, Mata and co-workers combined multiple bioactive epitopes to recreate key features of the bone ECM.[145] Specifically, they co-assembled three different PAs (one labelled with RGDS, one to promote osteogenesis and one to promote angiogenesis) with pro-angiogenic polymeric tyramine-modified hyaluronic acid. By culturing human adipose-derived mesenchymal stem cells (hAMSCs) and HUVECs, it was shown that the hydrogel promoted cell adhesion as well as osteogenic and angiogenic differentiation in both 2D and 3D culture. Furthermore, HUVECs were shown to grow into vascular tubules, with bone-like constructs being created *in vitro*.

Clearly, combining LMWGs with PGs enables the tuning of properties to overcome weaknesses and harness the potential strengths of each individual component. Generally, this can be achieved *via* simple co-formulation. It remains important to carefully characterise each component within a hybrid gel and unambiguously determine its role, but this approach is a powerful and versatile way of achieving multi-functionality in self-assembled gels.

5.2 Incorporating bioactive agents into LMWG hydrogels

In the previous section, we described how biopolymers can be incorporated into LMWG hydrogels by co-formulation. A few examples hinted at how bioactive agents could be incorporated in gels to promote cell growth. We have also described how bioactive peptide sequences like RGD or IKVAV, can be incorporated into LMWG hydrogels. This section focusses on incorporating larger functional biomolecules to direct cell growth.

Liang and co-workers mixed Nap-FFY with two bioactive factors, stromal cell derived factor-1 (SDF-1) and bone morphogenetic protein (BMP-2), and hydrogels were formed (Fig. 16a).[146] SDF-1 plays a key role in recruitment and proliferation of stem cells, while BMP-2 promotes differentiation. The presence of the growth factors did not affect the mechanical performance of the gel, and they were released synchronously from the gel over a period of days, with release reaching a maximum after about 3 weeks. The Nap-FFY gel exhibited no cytotoxicity and accelerated proliferation of bone marrow mesenchymal stem cells (BMSCs). On its own, Nap-FFY could not promote MSC differentiation, but once loaded with the growth factors, MSCs exhibited significant levels of ALP expression, indicating osteogenesis. *In vivo* testing demonstrated the ability of the gel to regenerate periodontal bone in defect areas (Fig. 16b and c) and the authors suggested potential future use of this system in dentistry.

Working with sorbitol-based **DBS-CONHNH$_2$**, we incorporated polyanionic heparin, a growth promoter that can assist angiogenesis, to promote the growth of mouse embryonic

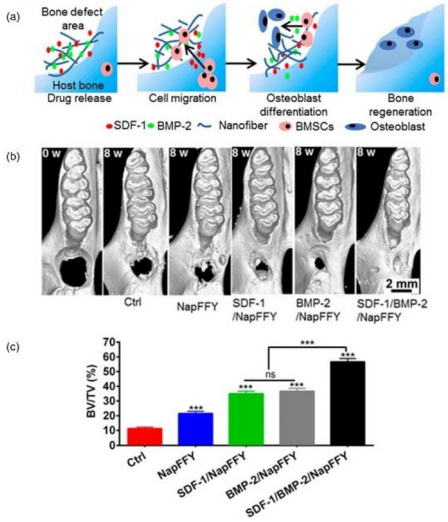

Fig. 16 (a) Schematic illustration of promoted periodontal bone regeneration by the SDF-1/BMP-2/NapFFY hydrogel in the bone defect area. Slowly released SDF-1 from the hydrogel recruits BMSCs to the defect area; then BMP-2 promotes BMSCs to differentiate into osteoblasts, initiating periodontal bone regeneration. (b) Micro-CT images of the periodontal bone defect areas in the maxillae of rats of different groups (size of each bone defect is about 20 mm^3). (c) Bone volume fractions of defect areas in different groups at 8 weeks. Data are expressed as mean ± SD, n = 3. Figure adapted from ref. 146 with permission of the American Chemical Society, copyright 2019.

fibroblast (3T3) cells.[77] We mixed heparin into **DBS-CONHNH$_2$** and also explored a hybrid hydrogel approach incorporating agarose as a secondary polymer gel network for mechanical reinforcement. The addition of heparin somewhat facilitated fibroblast growth, whereas the addition of agarose significantly decreased proliferation because of its high stiffness and lack of adhesion points. Heparin has also been loaded into larger RADA-based peptide hydrogels,[147] improving the binding of several growth factors such as VEGF165, TGF-β1 and FGFβ and slowing their release from the gel. Cell viability testing with HUVECs showed a significant effect of released VEGF165 and FGFβ on proliferation, with higher live cell numbers, demonstrating how multiple bioactive components can be incorporated in a gel and behave synergistically.

Kraatz and co-workers created a series of hydrogels based on C_{14}-FF, which were co-formulated with potential bioactive agents including carbohydrates, amino acids, vitamins, and hyaluronic acid building blocks.[148] When MSCs were grown in these gels, they were demonstrated to have high cell viability percentages, with the multi-component gels supporting slightly higher cell viability of MSCs than C_{14}-FF alone. It was suggested that more significant differences in long-term cell growth and differentiation might emerge in future studies.

Li and co-workers created hybrid hydrogels by combining Nap-FF with the biopolymer silk fibroin.[149] The presence of Nap-FF triggered a conformational transition of the silk fibroin from random coil to β-sheet *via* hydrogen-bonding and the hydrophobic effect. The researchers then used Nap-FFRGD with silk fibroin and found the resulting injectable hybrid hydrogel was compatible with HUVEC growth. When further loaded with vascular endothelial growth factor (VEGF) this gel caused cell morphogenesis because of the bioactive agent. When subcutaneously injected in mice this multi-component system triggered the generation of new blood capillaries *in vivo*, supporting microvasculature through coordinated interactions between HUVECs, VEGF and the gel matrix.

Shen and co-workers designed and synthesized a nanofibre hydrogel made of a larger peptide covalently attached to insulin-like growth factor-1, which is beneficial to cellular processes.[150] Rather than simple co-formulation, this uses a chemical covalent strategy to incorporate the bioactive agent. Although having the disadvantage of requiring more synthetic input, this strategy can unlock benefits of more precise incorporation, with the bioactive agent being permanently fixed in the gel at well-defined locations. In this case, the resulting gel was biodegradable and showed no toxicity to neural stem cells *in vitro* and *in vivo*, promoting stem cell proliferation and encouraging differentiation to neurons and oligodendrocytes. Importantly, the gel activated downstream IGF-1 signalling pathways because of the bioactive unit. Mixed with neural stem cells, this gel was implanted into lesion sites of spinal cord injuries in rats and regenerated neuronal and axonal cells, leading to the reconnection of damaged sites, generating neurite outgrowth and myelin sheath regeneration.

This section has emphasised the relative ease with which bioactive agents can be formulated into LMWG hydrogels and the benefits this can bring. Currently, it is evident that the bioactive agent often dominates the overall performance. Increasingly, it will be important to demonstrate specific advantages of the LMWG scaffold and to develop predictive rules that allow the optimal LMWG to be identified in each case.

6 Engineering LMWG hydrogels to enhance stem cell growth

Thus far, we have focussed on the chemical structure and properties of the gels to understand how they interface with stem cells. However, it is also possible to 'engineer' gels using physical approaches to fabricate them in different ways. Gels can vary significantly in properties, performance and potential, dependent on how they have been made. This section explores how LMWG hydrogels can be engineered to achieve outcomes of potential importance in regenerative medicine.

6.1 Shaping and patterning LMWG hydrogels to direct stem cells

There is considerable interest in shaping and patterning gels for a wide range of applications.[151] Using shaped gels to support stem cell growth can potentially create more functional assemblies of cells. Furthermore, by introducing a degree of patterning, it is possible to generate materials in which cells behave differently on different domains, or in

which gradients in the gel can lead to cellular organisation. Such principles are established for polymer hydrogels,[152] but are only beginning to emerge for LMWG hydrogels. For LMWG hydrogels, shaping and patterning can sometimes be challenging because of their dynamic nature and relative rheological weakness.

6.1.1 Microscale moulded LMWG hydrogels. In their early work from 2007, Liebmann and co-workers reported that **Fmoc-FF** hydrogels could be made in patterned silicon microstructured chambers, originally designed for use in microfluidic devices.[48] Hydrogels were formed from aqueous cell suspensions and in the resulting 3D culture, the mammalian cells retained a rounded morphology, in contrast to the spread morphologies observed when cultured on 2D surfaces like glass. Within these moulds, the gel could also be broken down by flow-generated shear stress, pH modification (pH 9.0 and above), or enzyme digestion, although this process was not fully optimised. The authors suggested that the reversibility of LMWG hydrogels offered a potential advantage for developing reusable microscale platforms for tissue culture.

6.1.2 Macroscopic gel beads. In the early 2020s, we developed methodologies to produce millimetre-scale LMWG hydrogel beads *via* co-formulation of an LMWG with a stabilising PG such as calcium alginate or agarose, which helps the final beads to retain their integrity.[153,154] This is a powerful application of the co-formulation hybrid LMWG/PG strategy (see section 5.1). With an interest in stem cell growth, **DBS-CONHNH$_2$** was mixed with alginic acid, glucono-δ-lactone (GdL) and calcium carbonate (Fig. 17a) in hot water, and added as droplets with defined size into cold paraffin (Fig. 17b).[155] The LMWG rapidly assembled on cooling, and then, more slowly, as the pH was lowered by hydrolysis of GdL, Ca^{2+} ions were solubilised, crosslinking the alginate PG network, stabilising the millimetre-scale hybrid hydrogel beads (Fig. 17c). Importantly, hMSCs had excellent compatibility with these beads and we argued that the relatively high surface areas encouraged cell growth, adhesion and penetration. Clearly there is future potential to create structured 'organoid'-type cell cultures.

One of the unique chemical features of **DBS-CONHNH$_2$** is that it reduces precious metals *in situ* to yield metal nanoparticles, while itself being oxidised to DBS-CO_2H.[156] We exposed the hybrid hydrogel beads to $AgNO_3$ and hence loaded them with silver nanoparticles (AgNPs) (Fig. 17d). These AgNPs exhibited antimicrobial properties, with the gels being active against challenging bacterial strains such as Vancomycin-resistant *Enterococcus faecium* (VRE) and *Pseudomonas aeruginosa*. Interestingly, at lower AgNP loadings, stem cell growth was also maintained. It was argued that careful optimisation would allow the fabrication of gels for potential post-surgical applications, supporting tissue regrowth whilst preventing opportunistic infections. A similar approach was applied using gellan gum as the PG.[157] This led to hybrid hydrogel beads with exceptional stiffness (G' = 46600 Pa), which retained excellent hMSC compatibility. Such materials may have potential use in orthopaedic applications.

6.1.3 Gel micro/nano-particles controlled *via* emulsion methods. It is also possible to fabricate LMWG hydrogel beads with much smaller diameters. In 2011, Collier and co-workers used a hydrogel based on a self-assembling peptide 11-mer to fabricate spherical microgels.[158] An aqueous solution of peptide was homogenised in oil to form an emulsion with microsized aqueous particles. The gelator is salt-sensitive, and the addition of PBS buffer triggered assembly, leading to self-assembled peptide microgels. Particle diameters were dependent on stirring rate, being tuned from 1.5–35 μm. This process was compatible with cell growth and allowed NIH 3T3 fibroblasts or C3H10T-1/2 mouse pluripotent stem cells to be encapsulated in the microspheres. After encapsulation, the microgels maintained cell viability, clearly demonstrating how

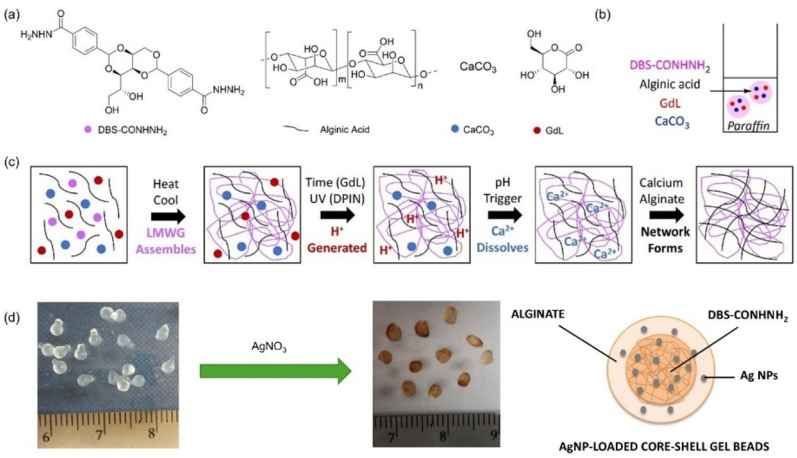

Fig. 17 (a) Components used in the formation of hybrid hydrogel beads. (b) Schematic of fabrication method for gel beads based on dropwise addition of a hot solution of the mixture of components to cold paraffin. (c) Schematic of the stepwise assembly process taking place within the gel beads. (d) Photograph of the gel beads, and scheme illustrating how treatment with $AgNO_3$ leads to loading of AgNPs into the gel beads. Figure adapted from ref. 155 with permission of the American Chemical Society, copyright 2022.

gel engineering and fabrication technology can be combined with cell growth to yield shaped gel-cell constructs.

In 2021, we combined **DBS-CONHNH$_2$** as LMWG, with calcium alginate PG to generate reinforced nanogel particles.[159] Hot **DBS-CONHNH$_2$**/alginic acid was added dropwise to cold paraffin oil to trigger **DBS-CONHNH$_2$** assembly, with rapid stirring and the presence of Span 80 surfactant ensuring LMWG assembly occurred within dispersed emulsion droplets. After 1 h, $CaCl_2$ was added to crosslink the alginate and form the PG network, stabilising the LMWG nanogel particles (diameters *ca.* 800 nm). The gel nanospheres could be stored for extended periods in solution without aggregation or degradation and injected through a standard medical-gauge needle without damage. The nanogels were also loaded with heparin, and it was demonstrated that nanogel-mediated heparin release enhanced hMSC growth. It was suggested that such nanogels may have future applications as injectable tissue repair agents.

6.1.4 3D-printing by extrusion. The ability to shape LMWG hydrogels by printing methods based on extrusion has significant potential due to its relative practical ease, allowing the fabrication of 3D objects. Bioprinting is increasingly widespread, particularly common with polymeric systems, and is a desirable, simple, reproducible methodology for gel shaping.[160] Although synthetic and natural polymer hydrogels are typically used in 3D-printing, there are limitations, particularly a lack of biological compatibility, poor rheological properties, or undesirable degradation profiles under physiological conditions.[161] There has therefore been emerging interest in 3D-printing LMWG hydrogels for cell growth applications. The most common approach to 3D-printing gels is simple extrusion in which a gel is formed, extruded through a needle as a solution, then reassembled *in situ* on the printing substrate.

Barthélémy and co-workers developed a nucleotide lipid (Fig. 18a) hydrogel as a potential new bioink for extrusion printing.[162] This LMWG formed self-supporting nanofibrillar hydrogels (Fig. 18b) in cell culture media and could be 3D-printed in the presence of cells under physiological conditions (Fig. 18c and d). *In vitro* studies with human gingival fibroblasts and stem cells from the apical papilla indicated that the cells could survive extrusion. Fibroblasts had higher cell viability with an increase in metabolic activity over time, while stem cell viability decreased – this likely reflects the greater stability of fibroblasts compared to stem cells described earlier. The printed gel was also shown to have *in vivo* compatibility and demonstrated slow biodegradation over days-weeks.

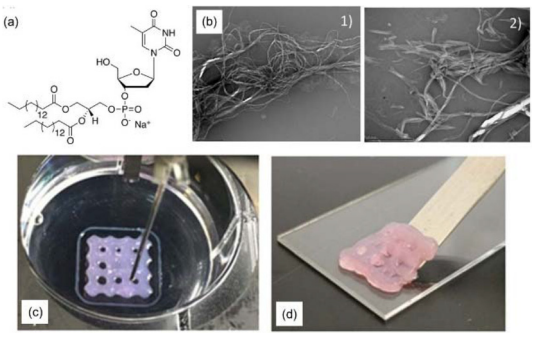

Fig. 18 (a) Chemical structure of diC_{16}dT nucleotide lipid LMWG used in extrusion printing. (b) TEM images of diC_{16}dT hydrogel (3% wt/vol) in culture medium (DMEM, with 123.5 mM NaCl final concentration): (1) scale bar 2 μm; (2) scale bar 1 μm. (c) Bioprinted lattices (1 printed layer) of diC_{16}dT hydrogel in culture medium. (d) Completed bioprinted lattice of diC_{16}dT (3% wt/vol) in culture medium showing some flexibility. Figure adapted from ref. 162 with permission of Springer Nature, copyright 2020.

Perez and co-workers reported a hydrogel derived from co-assembly of guanosine and guanosine 5′-monophosphate with potassium ions and boronic acid and developed it for use as a bioink.[163] Guanosine and guanosine 5′-monophosphate co-assemble into G quartets and the significant difference in their relative solubilities allowed tuning the ratio to form a hydrogel near physiological pH. A 1 : 1 ratio was optimal for 3D bioprinting, and once printing was complete, hyperbranched polyethylenimine was added to coat the printed hydrogel, increasing its stability for cell culture. Rat MSCs were viable on the printed support, with MSC numbers increasing over time if cells were printed alongside the LMWG. The cells displayed rounded morphology after 21 days, and when cultured in adipogenic media, lipid droplets were detected, suggesting adipogenic differentiation in the printed hydrogel.

Working with BTA monomers and dimers (see section 2.3.4), Baker and co-workers developed a tunable gel by modifying the hydrophobic substituents on the BTA monomer, enabling the viscoelastic properties of the gel to be varied over 5 orders of magnitude, allowing it to be optimised for 3D-printability.[164] In particular, the stress relaxation, which indicates the ability of the gel to dissipate stress on the network level, was tuned. Chondrocytes exhibited good cell viability in both bulk and bioprinted hydrogels, and hMSCs were able to form spheroids over the course of cell culture. It was suggested that conventional polymer hydrogels with static cross-links which can limit cell–cell interactions, often prevent spheroid formation, while dynamic LMWG systems such as this one can potentially better facilitate hMSC spheroid formation.

Using larger peptides with hydrophobic/hydrophilic domains, Hartgerink and co-workers optimised the structures as inks to create complex 3D structures including co-printing multiple gelators with layered structures, overhangs, and internal porosity.[165] Peptides incorporating positively charged lysine or negatively charged glutamic acid could be printed alongside one another and the multi-component printed constructs induced differences in the behaviour of C2C12 myoblasts typically used to study muscle behaviour.

6.1.5 Gel 'noodles'. Some of the earliest work to shape molecular gels focussed on fabricating gel shapes described as 'noodles'. In 2010, Stupp and co-workers developed a strategy for achieving gel 'noodles' based on their PA hydrogels.[166] This approach used heating to achieve liquid crystalline alignment of cylindrical micelles. When dragged from a pipette onto salty media, this created noodle-shaped gel strings as the

salt triggered charge screening of the cylindrical micelles (Fig. 19a). Not only were these noodles shaped, but they also had a good degree of alignment of the gel nanofibres within them (Fig. 19b).

It was reported that hMSCs were compatible with the noodle-forming process and could be encapsulated – they also became aligned (Fig. 19c). Long-range cell alignment has great potential in terms of enabling cells to communicate over distances. The authors incorporated HL-1 cardiomyocytes, a cell line with spontaneous electrical activity that requires extensive cell–cell contacts to propagate signals and found they proliferated to fill the entire structure. By fluorescently visualizing intracellular calcium concentration, pockets of spontaneous electrical activity were observed by day 6, and by day 10 action potentials could propagate through the entire macroscopic structure (Fig. 19d). The authors highlighted the potential of these 'cellular wires' in regenerative medicine applications such as the treatment of cardiac arrhythmia.

Others have applied this approach to gel noodle formation to ultra-short peptide LMWG hydrogels, again demonstrating internal nanofibrillar alignment.[167] Very recently, Adams and co-workers described the use of controlled mechanical inputs to manipulate the thickness of sections of the gel noodles. They found that C2C12 myoblast cultures showed improved cell adhesion, elongation, and myogenic differentiation on the thin segments of the noodles, compared to the thicker segments, with potential application in muscle regeneration.[168]

6.1.6 3D-printing by wet-spinning. Fitremann and co-workers developed wet-spinning methods for the 3D-printing of LMWG hydrogels. In wet-spinning, an LMWG is dissolved in a 'good' solvent (*e.g.* DMSO), and then injected, under controlled conditions into a 'bad' solvent (*e.g.* H_2O) (Fig. 20a and c).[169] This is conceptually related to noodle formation described above, but noodles more often use salt solutions as coagulants rather than a solvent switch. Wet-spinning, as described by Fitremann, is fully automated and highly reproducible. If the assembly kinetics are aligned with injection kinetics, this results in the formation of a well-defined gel filament (Fig. 20b). If printed from a moving needle, these gel filaments fall to the bottom of the bath and can be printed in multiple layers to give well-defined 3D objects.

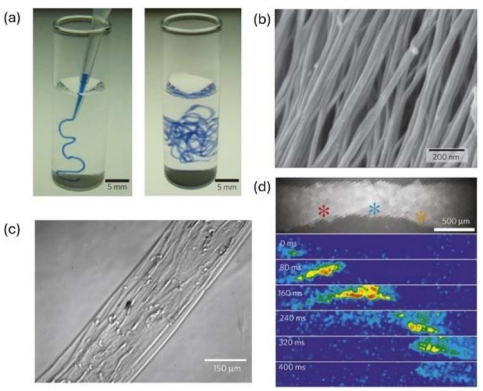

Fig. 19 (a) PA solution coloured with trypan blue injected into phosphate-buffered saline after heat treatment. (b) Aligned nanofibre bundles in strings formed by dragging thermally treated PA solutions onto a $CaCl_2$ solution. (c) Preferential alignment of encapsulated hMSCs along the string axis. (d) Top: calcium fluorescence image of HL-1 cardiomyocytes encapsulated in noodle-like string. Bottom: successive spatial maps of calcium fluorescence intensity at 80 ms intervals, showing propagation of an electrical signal through the string. Figure adapted from ref. 166 with permission of Springer Nature, copyright 2010.

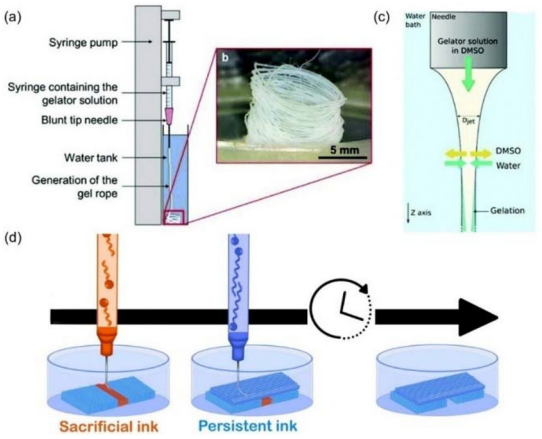

Fig. 20 (a) Experimental set-up for wet-spinning based on injection of a solution of LMWG into water to produce a wet-spun filament. (b) Photograph of wet-spun filament produced from **Gal-C7**. (c) Schematic of wet-spinning process indicating how solvent exchange drives gel assembly within the extruded solvent column. (d) Experimental set up for wet-spinning with two different LMWGs – one sacrificial and one persistent, in order to create a patterned wet-spun 3D-printed morphology that evolves over time. Figures adapted from ref. 169 and 170 with permission of the Royal Society of Chemistry, copyright 2019, and Elsevier, copyright 2022, respectively.

In their initial work, Fitremann and co-workers used **Gal-C7** (see section 2.3.2) as the LMWG, but the wet-spun objects were not compatible with the growth of neuronal cells.[169,171] This was assigned to the relative rheological weakness of the printed objects, resulting from the significant water solubility of the LMWG. Fitremann and co-workers went on to replace **Gal-C7** with Gal-C9 and demonstrated that the more stable self-assembly of the more hydrophobic Gal-C9 significantly improved the stability of the printed objects.[74] In this case, although hMSCs were stable on bulk Gal-C9 gels with a fibrillar structure formed *via* a heat-cool cycle, the 3D-printed hydrogels, where the microstructure is composed of micrometric flakes, appeared too fragile to withstand cell growth.[170] This emphasises the fact that cell growth does not only depend on LMWG structure, but also on nanoscale morphology and bulk gel properties, which can vary depending on the way the LMWG hydrogel has been fabricated. This is a topic we return to in section 6.2.2. Fitremann and co-workers went on to use the different stabilities of **Gal-C7** and Gal-C9 to print objects containing both LMWGs in which the more soluble gelator (**Gal-C7**) acted as a 'sacrificial ink' – as it dissolved from the printed objects, it left channels within the

more stable 'persistent ink' (Gal-C9) (Fig. 20d). Temporal evolution, such as that observed in these dynamic materials, is of key current interest in LMWG hydrogel science, ultimately having potential for '4D' control over stem cell growth (see section 6.3).

Working in collaboration with Fitremann, we applied wet-spinning to 3D-print our well-established **DBS-CONHNH$_2$** LMWG.[78] The printed objects had a fibrillar morphology equivalent to that observed in the bulk gels, with excellent stability in aqueous solution over extended periods of time, suitable for cell culture. As described above, **DBS-CONHNH$_2$** can reduce precious metals *in situ* to give metal nanoparticles.[156] This unique behaviour is programmed into the 3D-printed objects based on this LMWG. **DBS-CONHNH$_2$** with embedded AuNPs had excellent compatibility with Y201 hMSCs, with the presence of AuNPs enhancing stem cell proliferation. The positive impact of AuNPs on stem cell growth is proposed to result from their ability to act as cues that activate key intracellular signalling pathways (see section 6.1.8).

6.1.7 Photopatterning. In 2014, we developed a methodology to photopattern multidomain hybrid LMWG/PG hydrogels *via* self-assembly of an LMWG and subsequent photopolymerization of the PG using a mask to create domains with different compositions,[172] which we went on to apply for controlled release.[173]

In a landmark study, He and co-workers used this approach to fabricate a multi-domain hybrid hydrogel for tissue engineering.[174] They employed a peptide LMWG and selected poly(ethylene glycol) diacrylate (PEGDA) as the photopolymerisable PG (Fig. 21a). Performing photopolymerisation through a mask polymerised rigid domains of PG within the softer LMWG matrix. Careful characterization of the interface regions between gel domains indicated interpenetrating LMWG and PG networks of intermediate stiffness, with a unique gradient of mechanical properties across the interface. MSCs can proliferate and migrate into the gel matrix. In the softer LMWG domain, MSCs undergo chondrogenic differentiation while osteogenic differentiation occurred on the stiffer domain where the PG has been crosslinked (Fig. 21b). Excitingly, the interface between LMWG and PG could direct osteochondral regeneration (cartilage and subchondral bone). This indicates how interface regions can be created in patterned multidomain gels with exquisite control, allowing cells to take on more complex, tissue-like structures.

We also recently reported the use of this approach to create hybrid hydrogels based on the combination of an LMWG (**DBS-CONHNH$_2$**) with poly(ethylene glycol) dimethacrylate (PEGDM).[175] In this case, the bioactive growth factor promoter heparin was also incorporated. The hybrid gel somewhat restricted heparin release because of the interpenetrated networks. The multicomponent system was photopatterned within a well-plate under a mask to yield gels with a softer half and a stiffer half ready for cell culture. Confocal microscopy using fluorescent hMSCs indicated the stem cells grew much more effectively on the softer domain in the absence of cross-linked PEGDM leading to spatially controlled cell growth on the multi-domain gel because of the photopatterning.

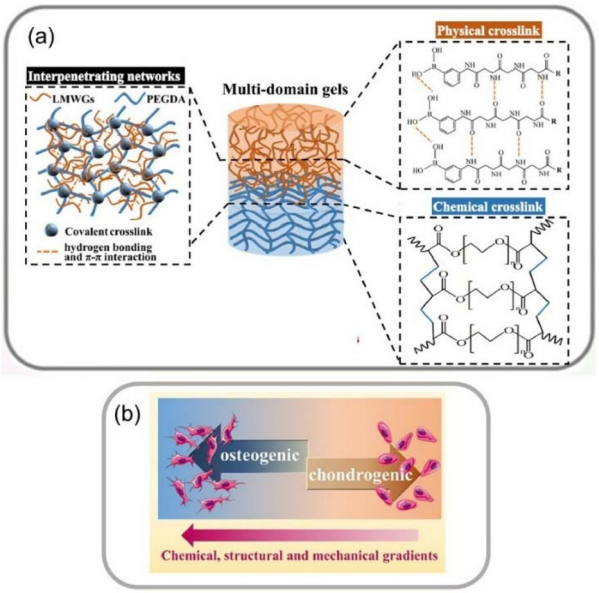

Fig. 21 (a) Multi-domain gel in which the softer domain (peach) is assembled from physically crosslinked LMWGs, while the stiffer domain (blue) consists of a chemically crosslinked PG triggered by photopolymerisation. There is a degree of network overlap in the interface region. (b) Stem cell growth responds to the mechanical properties of the different domains, with chemical, structural and mechanical gradients existing within the patterned material. Figure adapted from ref. 174 with permission of Elsevier, copyright 2021.

6.1.8 Patterning by diffusion/stamping. Diffusion is an interesting strategy for patterning self-assembled LMWGs. The dynamic nature of self-assembled gels opens unique possibilities both for spatial patterning, but also to achieve temporal control over gel behaviour (see section 6.3). To exemplify the potential of diffusion to spatially-resolve gels and hence influence stem cell growth, we developed a simple, innovative approach to patterning **DBS-CONHNH$_2$**.[176] Paper stamps were loaded with Au(III) solution and placed on top of a hybrid hydrogel combining the LMWG with gellan gum as a reinforcing PG (Fig. 22). As Au(III) diffuses into the gel, it encounters the LMWG and is reduced to Au(0). This led to easily visualised purple-coloured AuNP patterns in the **DBS-CONHNH$_2$** gel. The concentration of Au(III) loaded into the paper controlled the lateral spatial resolution and the depth of patterning.

When hMSCs were grown on these patterned gels, much better cell adhesion was observed on the AuNP-loaded domains, with spread cell morphologies. In contrast, in the unpatterned parts of the gel only composed of **DBS-CONHNH$_2$** and gellan gum, hMSC proliferation was lower, with rounded cell morphologies. ALP expression measurements proved that osteogenesis was taking place on the patterned domain, but not in the unpatterned regions. The ability of AuNPs to promote osteogenesis results from their involvement in intracellular signalling pathways, such as p38 MAPK and Wnt/

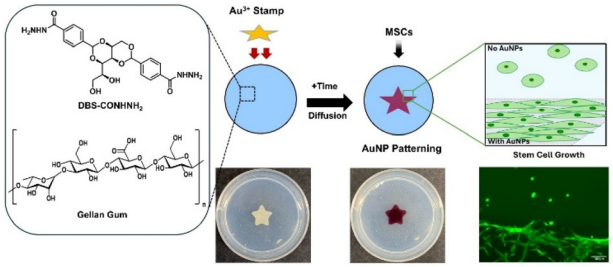

Fig. 22 Schematic of gold nanoparticle (AuNP) patterning on hybrid hydrogel based on **DBS-CONHNH$_2$** and Gellan Gum (GG). Star-shaped filter paper loaded with Au(III) is placed on the hydrogel (photograph below), and Au(III) diffuses out, resulting in AuNP formation *in situ* and resultant gel patterning (photograph below). hMSCs cultured on the AuNP-loaded domain show differences in cell proliferation and morphology, having high proliferation and spread shapes, with evidence of osteogenesis compared with the unpatterned domain which exhibits lower proliferation and rounded cell shapes (confocal microscopy image of hMSCs at day 6 stained with calcein AM). Figure adapted from ref. 176 with permission of Wiley-VCH, copyright 2025.

β-catenin. This simple patterning approach thus generates LMWG hydrogels in which the fates of stem cells are under precise spatial control.

Pires and co-workers demonstrated that a glycosylated peptide LMWG could support the growth of cardiomyocytes, enabling efficient electrical interconnectivity, with potential applications in cardiac tissue regeneration.[177] The researchers micropatterned the LMWG by placing a polydimethylsiloxane (PDMS) stamp with parallel grooves onto the gel, and applying low pressure. This simple physical stamping approach created a pattern with grooves 15 μm wide and 5 μm deep – these were used to culture and promote alignment of pluripotent stem cell-derived cardiomyocytes. Cardiac markers including gap junction protein connexin-43, cardiac troponin T and sarcomeric-α-actinin were detected, and the cultured cells exhibited anisotropic synchronized contractions, indicating electrical interconnectivity. Patterning was shown to enhance cell elongation, providing the anisotropy required in cardiac tissue.

6.2 Using gel fabrication method to tune hydrogel performance

6.2.1 Cell-compatible gel fabrication. Depending on how LMWGs are assembled into hydrogels, the resulting materials can have very different properties. For example, fabricating a gel and subsequently loading it with cells can have different cell culture outcomes compared to triggering gel formation in the presence of cells. The former approach starts off as a 2D culture on the gel surface, and requires invasion of the cells into the gel, while the latter can create 3D cell culture *in situ.* However, many LMWGs are triggered by stimuli that are not easily compatible with cell growth and do not allow the cells to be present during gel preparation, hindering simple cell encapsulation. Although examples where 3D culture is possible have been presented earlier in this review, it is nonetheless worth giving careful thought to the way an LMWG hydrogel is fabricated to optimise the possibility of effective 3D cell culture. A number of LMWGs require an extreme temperature cycle to assemble into a gel, limiting cell compatibility and preventing injection *in vivo*. If the gels can instead be formed by triggering gel formation with (*e.g.*) salts or cell culture, it can become possible to mix a cell suspension with the LMWG during gel formation, resulting in cell encapsulation.

With the goal of enabling 3D cell culture, Collier and co-workers modified their larger peptide gelators to make them more amenable to gel fabrication in the presence of cells.[178] Their previous peptides required a low pH (*ca.* pH 3) to dissolve prior to assembly. The peptide was modified by incorporating a Gln-Glu unit, introducing negative charge at physiological pH, meaning it dissolved more effectively. This enabled hydrogel assembly in the presence of cells and was used by to culture prostate cancer cells. Although cancer cells are not the primary focus of this review, this study aimed to create 'healthy' cancer spheroids based on the tumour from an individual patient as models of disease for use in personalised medicine, determining optimum treatment regimes. Similarly, Grabowska and co-workers used a FEFEFKFK peptide hydrogel as a 3D model to culture breast cancer patient-derived xenografts (PDXs).[179] The cancer cells grew and formed clusters in the gel, allowing the development of 3D disease models designed to test drug sensitivity.

Tomasini and co-workers demonstrated how thixotropic LMWG hydrogels facilitate cell encapsulation.[180] Their gel based on a simple peptide binding to calcium ions could assemble in Dulbecco's modified Eagle's medium (DMEM) supplemented with 1% fetal calf serum (FCS), penicillin (50 UI mL^{-1}), and streptomycin (0.05 mg mL^{-1}), and on simple shaking broke into a sol before re-assembling. Incorporating human fibroblasts after shaking allowed them to be encapsulated within the gel, which reformed around the cells. Kieltyka and co-workers also used thixotropy to load hiPSCs into synthetic LMWG hydrogels based on a triamine functionalised with squaramides and peripheral PEG chains.[181] Gentle pipetting broke the gel and allowed stem cells to be introduced. Furthermore, dilution enabled the gentle release of individual cells from the gel. This highlights the advantages that supramolecular systems can exhibit in terms of cell encapsulation and release if they possess reversible thixotropic character.

6.2.2 Changing gel properties by fabrication method. It should be noted, however, that changing gel assembly method can have profound and unexpected impacts on the resulting gel, which must be considered when developing self-assembling LMWG hydrogels for any sort of application. Most self-assembled gels are kinetically trapped materials with metastable structures as a result of the processing imposed on them. The 'history' of an LMWG hydrogel can play a pivotal role in directing how LMWGs assembles at the molecular-scale, or in terms of modifying the nanoscale morphology and rheological performance.[182,183] Great care is therefore required in the way these materials are handled/produced in order to achieve reproducible results.[184] However, this variability also

introduces an alternative mechanism through which the performance of bioactive LMWG hydrogels can potentially be controlled.

As an example of the impact of gel fabrication, Roy and co-workers formed two-component hydrogels by mixing carboxybenzyl-protected diphenylalanine (Cbz-FF) and serine (Cbz-S).[185] The ratios were varied, and gel formation induced either using a heat-cool cycle or by sonication. Using the heat-cool approach, networks of long thin fibres were formed which gave stiffer hydrogels, whereas sonication gave rise to flat-twisted nanofibers and a softer gel. As such, these materials were tunable both in terms of the co-assembly of Cbz-FF and Cbz-S, and the chosen fabrication method. The viability of mouse fibroblasts (L929) improved when a higher ratio of hydrophilic Cbz-S was present. In terms of gel fabrication method, there was higher cell adhesion, viability and proliferation in gels formed *via* heat-cool cycles, even though the chemical composition was exactly the same as when sonication was used. This highlights the importance of controlling and understanding all levels of supramolecular assembly, molecular, nanoscale and network, to direct cell growth successfully using LMWG hydrogel materials.

6.3 Dynamic assembly – towards 4D control of cell growth

A key advantage of LMWG hydrogels in tissue culture is their dynamic, responsive nature. For example, there is potential for the gel scaffold to break down, either in a stepwise or a triggered manner at a defined timepoint – this can limit biopersistence or enable controlled release of encapsulated growth factors or tissues. Furthermore, the self-assembled nature of LMWG hydrogels gives them the potential to adapt and change their structures over time, either as a result of their inherent metastable nature or in response to stimuli. This opens the possibility of scaffolds that interact with cells in different ways at different timepoints. If combined with 3D spatial control over cell growth *via* shaping and patterning strategies (see section 6.1), this unlocks the possibility of '4D' control over tissue culture. Although increasingly well-established for polymer gels,[186,187] the development of 4D methods for tissue engineering using LMWG hydrogels remains a nascent and exciting field of research, perfectly poised to take advantage of the unique dynamic potential of this class of material.

6.3.1 Controlled gel disassembly. Although there are numerous reports of cell growth in LMWG hydrogels, examples in which the cells are extracted from the support at the end of cell culture remain relatively limited. It is perhaps surprising, given the reversibility of LMWG gels is an often-cited key potential advantage of their use in a biological setting. Although some examples were presented earlier in the article, it is worth considering why disassembly is relatively rare. Primarily, it is because LMWG gels are often disassembled by stimuli such as heating or a significant pH change, which would be detrimental to sensitive cultured cells.

In 2012, Yang and co-workers reported a peptide LMWG modified with an adamantane as the N-terminal hydrophobic unit.[188] Having demonstrated it was compatible with mouse fibroblast 3T3 cells, they went on to show that the addition of methyl-β-cyclodextrin (M-β-CD) could break down the gel and release the cells. This is a result of selective binding between M-β-CD and the adamantane unit driving gel disassembly, a supramolecular approach to gel breakdown. This has clear benefits when further study of individual cells is required after cell culture, and the authors commented on the relevance of such materials to studies of stem cell differentiation.

In 2024, an elegant example of stem cell release from a PA hydrogel was reported by Mata and co-workers.[189] To initially form the gels, the glutamic acid (pK_a = 4.25) in the PA was deprotonated, and gelation induced by the addition of metal ions, which coordinate with the glutamate unit (Fig. 23a). To disassemble the hydrogel, tetrasodium ethylenediamine tetraacetic acid (Na_4EDTA) was added. This chelates metal ions and hence breaks apart the self-assembled metal-coordinated nanostructure (Fig. 23b). Three different methods were used for cell retrieval – Na_4EDTA, enzymatic degradation and mechanical disruption by pipetting. More cells were retrieved when using Na_4EDTA, and cell viability was also higher. This recent work clearly demonstrates how developing simple cytocompatible triggers for gel disassembly remains of importance.

Demonstrating a different type of triggered response, Zhang and co-workers developed a photo-responsive peptide LMWG for use with hMSCs.[190] UV exposure induced the structural transformation of the tetrazole moiety in the LMWG to yield a fluorescent pyrazoline cycloadduct. This disrupted π–π interactions in the supramolecular structure and hence disassembled the gel. The researchers also demonstrated that photoirradiation through a photomask to pattern the gel could release encapsulated horse serum from the UV-exposed domain. This is known to lead to the differentiation of mouse myoblast C2C12 cells cultured in 2D on top of the gel. Furthermore, hMSCs grown in 3D within the gel exhibited

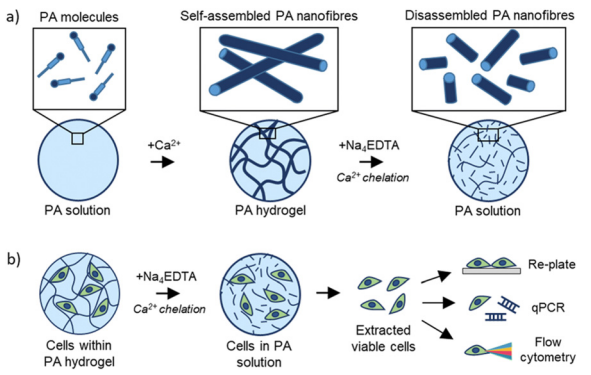

Fig. 23 (a) Schematics of **PA-E3** molecules self-assembling through interaction with $CaCl_2$ and disassembling on addition of Na_4EDTA which binds to calcium ions through chelation. (b) **PA-E3** hydrogels are disassembled to retrieve encapsulated cells for downstream biological analyses. Figure adapted from ref. 189 with permission from the Royal Society of Chemistry, copyright 2024.

morphologies with greater spreading after a short period of UV irradiation, which was assigned to the photo-induced change in the hydrogel matrix.

6.3.2 Dynamic processes within LMWG hydrogels. In order to start exploring the dynamic evolution of gel scaffolds over time, Das and co-workers recently presented the dissipative self-assembly of a peptide-based LMWG capable of supporting stem cell growth (Fig. 24).[191] Dissipative self-assembly occurs when non-assembling building blocks are activated by a chemical 'fuel' to obtain an active gelator, which subsequently assembles into a gel. However, once the fuel is exhausted, the chemical reaction is reversed, and the active LMWG is converted back into the precursor, leading to gel disassembly. The transient fuelled nature of dissipative gels mimics the dynamic aspects of many assembly processes found in nature.[192] In Das's work, a lipase enzyme catalysed esterification between *p*-hydroxybenzyl alcohol and a peptide bolaamphiphile, forming a monoester and then a diester. The diester is the active LMWG, and assembles to form thixotropic nanofibrillar hydrogels, a process that took place over several days. As the alcohol became depleted, the diester then hydrolysed, and the gel broke down. The authors demonstrated that this hydrogel could be used as scaffold to support human umbilical cord stem cell proliferation. However, they did not couple the dynamic properties of the gel to cell growth outcomes – to achieve this would begin to allow soft materials to exert temporal control over cell growth and potentially harness the unique potential of these dynamic gel-phase materials by interfacing them with dynamic biological tissue.

More recently, Das and co-workers explored a conceptually related dissipative system based on G-quartet assembly in which a modified guanine unit could undergo lipase-mediated esterification on its carboxylic acid chain terminus, activating the building block towards self-assembly.[193] In this work, they applied the scratch wound test to assess cell migration capacity. Cells were cultivated in a 24-well cell culture plate for 24 h, then a scratch was made using a sterile 200 μL tip and treated with the dynamic hydrogel. Fibroblasts were observed to migrate into the wound area for 24 h after treatment with the hydrogel (0.25 or 0.5 mM), with greater wound closure at higher loading.

Dynamic processes lie at the frontiers of self-assembled materials and offer a unique advantage of LMWG hydrogels in comparison to more static polymer systems. However, such processes are relatively challenging to measure and control. It is perhaps surprising given rapid current progress in this field of research, that very few studies have tried to use such materials with cells, and as yet, dissipative assembly has not been directly coupled to cell growth. It seems likely that processes coupling diffusion and dynamic exchange to stem cell growth outcomes at defined timepoints will become of increasing importance in developing next-generation cell growth scaffolds.

6.3.3 Bioresponsive hydrogel assembly. The development of LMWG hydrogels triggered by enzymatically driven reactions has seen significant effort.[194] The enzyme typically drives a reaction that changes the solubility of an LMWG precursor, converting it into a form capable of self-assembly. Xu and co-workers have reviewed the significance of such processes within a cellular context.[195] Clearly, gels that can assemble in response to enzymes have the potential to exhibit dynamic characteristics in the presence of cells.

In 2019, Xu and co-workers demonstrated that cells could instruct the assembly of an intercellular gel network, to create a kind of extracellular matrix, enabling the formation of cell spheroids (Fig. 25).[196] The phosphopeptide LMWG assembles into gel nanofibres on partial dephosphorylation catalysed by enzymes (*e.g.* phosphatases) in the intracellular space. Working with HS-5 cells, an immortalized human bone marrow stromal cell line characterized by fibroblast-like morphology, sheets of these cells could be encouraged to form cell spheroids. The LMWG had several features enabling this: (i) dephosphorylation enables assembly, (ii) D-chirality endows proteolytic stability, and (iii) biotin conjugation incorporates a cell-surface targeting ligand. HS-5 cells were chosen because they express relatively low level of phosphatases and only synthesize 3D ECM slowly. After being treated with the LMWG precursor in the culture medium for 24 h, HS-5 cells formed 3D cell spheroids from a 2D cell sheet, while in the absence of the LMWG precursor, the cells remained as a 2D sheet. Adding analogues without (i) the biotin motif or (ii) the phosphate group, meant the HS-5 cells remained as a 2D sheet, demonstrating the importance of the bioactive cues built into the LMWG for controlling dynamic assembly. TEM confirmed assembly of fibrillar objects between cells, with the dynamic, morphological change being reminiscent of the cell-mediated dynamics of fibronectin (*i.e.*, from globular to fibrillar structures during unfolding processes). It was concluded that the

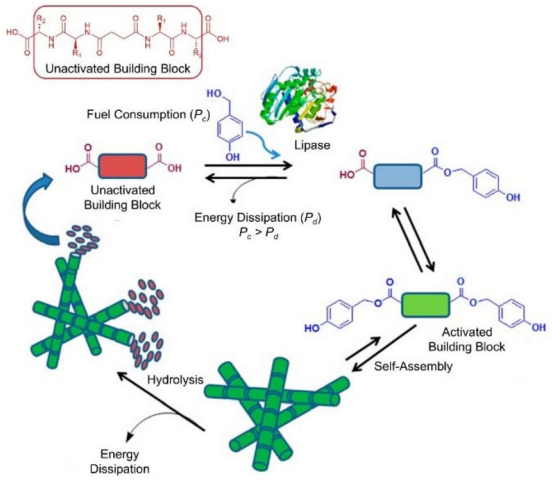

Fig. 24 Dissipative reaction cycle in which an unactivated peptide bolaamphiphile reacts with *p*-hydroxy benzylalcohol to give monoester then diester. The diester self-assembles into nanofibers and forms a hydrogel. Subsequent hydrolysis dissipates energy, resulting in hydrogel disassembly. If the rate of ester hydrolysis (P_d) is lower than that of esterification (P_c), the gel can form. Figure adapted from ref. 191 with permission from the American Chemical Society, copyright 2015.

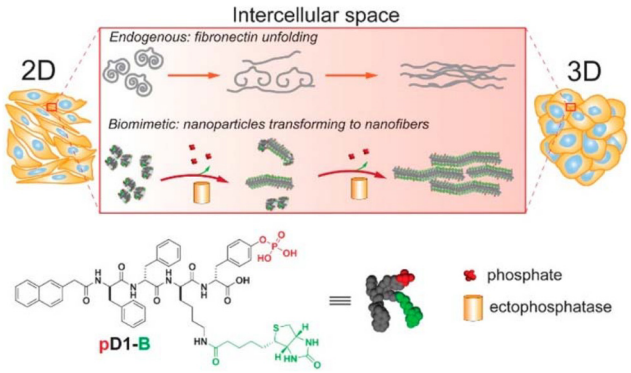

Fig. 25 Intercellular instructed-assembly of LMWG precursor (pD1-B) with enzymatically induced dephosphorylation leading to gel assembly and hence encouraging the conversion of 2D cell sheets into 3D spheroids. This process that mimics the essence of the dynamics of proteins such as fibronectin in the extracellular matrix. Figure adapted from ref. 196 with permission from the American Chemical Society, copyright 2019.

LMWG plays a biomimetic role in inducing formation of cell spheroids.

In 2023, Xu and co-workers further elaborated on this approach to gain full mechanistic understanding using a related LMWG precursor tagged with a fluorescent probe, enabling detailed microscopy.[197] Once again, this system induced intercellular nanofibres/gel assembly that potentially interact with fibronectin to enable cell spheroid formation. In this case, it was found that processes taking place within the cell played an integral role. Specifically, the D-phosphopeptide, being protease resistant, underwent endocytosis into the cell followed by endosomal dephosphorylation to generate helical nanofibres. On exocytotic secretion to the cell surface, these nanofibres then formed the intercellular gel that acts as an artificial matrix, facilitating fibrillogenesis of fibronectins and inducing cell spheroid formation. No spheroids were observed without *endo*- or exocytosis, phosphate triggers, or nanofibrillar morphology of the peptide assemblies.

This work clearly demonstrates how dynamic processes induced by biological cellular processes can be interfaced with gel assembly and that in turn, gel assembly can have a direct influence on the behaviour of the cell culture. It is anticipated that in future work, much progress can be made in the synergy between dynamic synthetic and biological systems to achieve tailored outcomes in terms of tissue engineering and regenerative medicine.

7 Conclusions and perspectives

In summary, LMWG hydrogels have significant value as extracellular matrix mimics capable of supporting the growth of stem cells, with potential applications in regenerative medicine.

A key advantage of LMWG hydrogels is the significant capacity for structural variation. Peptide LMWGs have perhaps the greatest range of tunability given the variability of amino acid building blocks and the high degree of non-covalent structuring afforded by the hydrogen bonding peptide backbone. Other biological building blocks also have hydrogen bonding groups to allow fibril assembly, can be easily modified, and offer an effective way of avoiding the hydrolytic degradation of peptides. However, perhaps the greatest structural advantage of the supramolecular approach to gel assembly is the ability to combine different LMWGs and hence create multi-functional materials taking advantage of either co-assembly or self-sorting strategies. This is a simple and effective way of enhancing the function of LMWG hydrogels at low synthetic cost, and allows facile tuning of mechanical properties, gel dynamics, or the incorporation of ligands to encourage cell adhesion, tags for imaging or other bioactive components into the gel network.

Chirality is a key structural characteristic that can tune the performance of LMWG hydrogels. In a simple sense, it can impact on biostability, preventing hydrolytic breakdown. However, the chirality of a gel, either at molecular or nanoscale levels can impact on cellular outcomes – clearly indicating that the self-assembling LMWG hydrogel can interact with chiral components within the cell, or important to cell growth and adhesion. Hierarchical assembly of LMWG hydrogels across multiple length-scales introduces unique possibilities to the ways in which these materials can interact with growing cells.

It is well-established that mechanical properties of gels can impact on stem cell growth, directing differentiation. Although demonstrated for LMWG hydrogels, it has still not been as widely explored as for PG hydrogels. However, one area in which LMWG hydrogels may surpass polymer systems is in terms of their dynamics. These materials express dynamic behaviour at both molecular and network levels that can impact on cell growth. Careful work is beginning to unpick the interplay between dynamic factors and mechanical characteristics in terms of directing stem cells. It seems likely that significant progress will be made in this area, and that 'ground rules' for the impacts of dynamics on stem cells will start to emerge.

Importantly, the need to understand non-covalent interactions across multiple length scales lies at the heart of developing a full understanding of the interface between LMWG hydrogels and stem cells. Both LMWG hydrogels and cells are inherently multi-scale materials, and understanding the interplay between these is essential. Therefore, as well as approaching transformative applications, research in this field has the potential to fundamentally innovate new principles in supramolecular science.

To extend the scope of LMWG hydrogels, co-formulation is a powerful strategy. Combining LMWG hydrogels with PGs or bioactive agents can harness the best of both types of material for directing stem cells. In future work, the structural variability and dynamic potential of LMWG hydrogels may both be used to significantly extend the performance of PGs and other active agents.

It is evident that extracellular matrix uses multiple different cues to simultaneously communicate with growing stem cells – mechanical, dynamic, chemical, biointeractive, *etc*. However, current LMWG hydrogels often remain limited to relatively simple single or dual signals. Multi-signal synergistic hydrogels represent a key frontier in the use of LMWG hydrogels for tissue engineering, however, untangling a detailed understanding of how such systems truly operate, and developing predictive capacity for soft materials design from first principles, will be significant fundamental challenges. It is possible that machine learning may offer approaches to gaining this type of insight across multiple complex systems.

Increasingly, attention is beginning to focus on how gels can be engineered to create more complex systems that achieve structured cell growth with a greater degree of complexity. For example, patterned materials can instruct stem cells to behave differently on different gel domains. This could help unlock *ex vivo* generation of more complex tissues ready for implantation. Clearly, new ways of shaping and patterning LMWG hydrogels have significant value. In addition, harnessing the dynamics of supramolecular materials, opens the possibility of 4D control over cell growth, in which the LMWG hydrogel evolves its composition or structure over time, and hence directs cells with a degree of temporal control. At present this is an unfulfilled target.

We therefore conclude that LMWG hydrogels have unique potential in tissue engineering and regenerative medicine. Some of the earliest gels based on larger peptides have already been commercialised as cell growth media, and therapeutic applications are under intense development. It is expected that smaller low-molecular-weight gelators will constitute the next generation of smart materials for tissue growth, benefitting from their low cost combined with easy incorporation of advanced functionality. By combining their unique structural characteristics with dynamics and gel engineering, we propose that LMWG hydrogels will become more closely mimetic of the extracellular matrix, and potentially offer capabilities that are not easily possible within natural systems, hence unlocking new vistas in tissue engineering and regenerative medicine.

Conflicts of interest

There are no conflicts to declare.

Data availability

This review article contains no novel data.

Acknowledgements

C. T. was funded by a scholarship from the Thai Government (AD039701).

References

1 S. Dong, S. An, Q. Saiding, Q. Chen, B. Liu, N. Kong, W. Chen and W. Tao, *Chem. Rev.*, 2025, **125**, 8835–8920.
2 W. He, M. Reaume, M. Hennenfent, B. P. Lee and R. Rajachar, *Biomater. Sci.*, 2020, **8**, 3248–3269.
3 C. D. Spicer, *Polym. Chem.*, 2020, **11**, 184–219.
4 H. Choi, W.-S. Choi and J.-O. Jeong, *Gels*, 2024, **10**, 693.
5 D. K. Smith, *Soft Matter*, 2024, **20**, 10–70.
6 L. Saunders and P. X. Ma, *Macromol. Biosci.*, 2019, **19**, 1800313.
7 K. J. Skilling, F. Citossi, T. D. Bradshaw, M. Ashford, B. Kellam and M. Marlow, *Org. Biomol. Chem.*, 2014, **10**, 237–256.
8 X. Du, J. Zhou, J. Shi and B. Xu, *Chem. Rev.*, 2015, **115**, 13165–13307.
9 L. Rijns, M. B. Baker and P. Y. W. Dankers, *J. Am. Chem. Soc.*, 2024, **146**, 17539–17558.
10 C.-M. Moysidou, C. Barberio and R. M. Owens, *Front. Bioeng. Biotechnol.*, 2021, **8**, 620962.
11 S. R. Caliari and J. A. Burdick, *Nat. Methods*, 2016, **13**, 405–414.
12 D.-C. Ding, W.-C. Shyu and S.-Z. Lin, *Cell Transplant.*, 2011, **20**, 5–14.
13 A. J. Friedenstein, *Acta Anat.*, 1961, **45**, 31–59.
14 A. J. Friedenstein, *Nature*, 1962, **194**, 698–699.
15 J. A. Thomson, J. Itskovitz-Eldor, S. S. Shapiro, M. A. Waknitz, J. J. Swiergiel, V. S. Marshall and J. M. Jones, *Science*, 1998, **282**, 1145–1147.
16 B. Lo and L. Parham, *Endocr. Rev.*, 2009, **30**, 204–213.
17 U. Kozlowska, A. Krawczenko, K. Futoma, T. Jurek, M. Rorat, D. Patrzalek and A. Klimczak, *World J. Stem Cells*, 2019, **11**, 347–374.
18 M. F. Pittenger, D. E. Discher, B. M. Péault, D. G. Phinney, J. M. Hare and A. I. Caplan, *npj Regener. Med.*, 2019, **4**, 22.
19 D. Deo, M. Marchioni and P. Rao, *Pharmaceutics*, 2022, **14**, 791.
20 A. J. Engler, S. Sen, H. L. Sweeney and D. E. Discher, *Cell*, 2006, **126**, 677–689.
21 M. D'Urso and N. A. Kurniawan, *Front. Bioeng. Biotechnol.*, 2020, **8**, 609653.
22 T. E. Ichim, P. O'Heeron and S. Kesari, *J. Transl. Med.*, 2018, **16**, 212.
23 P. Bainbridge, *J. Wound Care*, 2013, **22**, 407–412.
24 R. A. Denu, S. Nemcek, D. D. Bloom, A. D. Goodrich, J. Kim, D. F. Mosher and P. Hematti, *Acta Haematol.*, 2016, **136**, 85–97.
25 I. Greco, H. Machrafi, C. Minetti, C. Risaliti, A. Bandini, F. Cialdai, M. Monici and C. S. Iorio, *Int. J. Mol. Sci.*, 2024, **25**, 5600.
26 S. Zhang, T. C. Holmes, C. M. DiPersio, R. O. Hynes, X. Su and A. Rich, *Biomaterials*, 1995, **16**, 1385–1393.
27 T. C. Holmes, S. de Lacalle, X. Su, G. Liu, A. Rich and S. Zhang, *Proc. Natl. Acad. Sci. U. S. A.*, 2000, **97**, 6728–6733.

28 R. G. Ellis-Behnke, Y.-X. Liang, S.-W. You, D. K. C. Tay, S. Zhang, K.-F. So and G. E. Schneider, *Proc. Natl. Acad. Sci. U. S. A.*, 2006, **103**, 5054–5059.
29 G. A. Silva, C. Czeisler, K. L. Niece, E. Beniash, D. A. Harrington, J. A. Kessler and S. I. Stupp, *Science*, 2004, **303**, 1352–1355.
30 F. Gelain, D. Bottai, A. Vescovi and S. Zhang, *PLoS One*, 2006, **1**, e119.
31 C. Cunha, S. Panseri, O. Villa, D. Silva and F. Gelain, *Int. J. Nanomed.*, 2011, **6**, 943–955.
32 A. Aggeli, M. Bell, N. Boden, J. N. Keen, P. F. Knowles, T. C. McLeish, M. Pitkeathly and S. E. Radford, *Nature*, 1997, **386**, 259–262.
33 S. Maude, D. E. Miles, S. H. Felton, J. Ingram, L. M. Carrick, R. K. Wilcox, E. Ingham and A. Aggeli, *Soft Matter*, 2011, **7**, 8085–8099.
34 F. Gelain, Z. Luo and S. Zhang, *Chem. Rev.*, 2020, **120**, 13434–13460.
35 S. Sankar, K. O'Neill, M. B. D'Arc, F. Rebeca, M. Buffier, E. Aleksi, M. Fan, N. Matsuda, E. S. Gil and L. Spirio, *Front. Bioeng. Biotechnol.*, 2021, **9**, 679525.
36 F. Gelain, Z. Luo, M. Rioult and S. Zhang, *npj Regen. Med.*, 2021, **6**, 9.
37 M. P. Hendricks, K. Sato, L. C. Palmer and S. I. Stupp, *Acc. Chem. Res.*, 2017, **50**, 2440–2448.
38 V. M. Tysseling-Mattiace, V. Sahni, K. L. Niece, D. Birch, C. Czeisler, M. G. Fehlings, S. I. Stupp and J. A. Kessler, *J. Neurosci.*, 2008, **28**, 3814–3823.
39 A. J. Matsuoka, Z. A. Sayed, N. Stephanopoulos, E. J. Berns, A. R. Wadhwani, Z. D. Morrissey, D. M. Chadly, S. Kobayashi, A. N. Edelbrock, T. Mashimo, C. A. Miller, T. L. McGuire, S. I. Stupp and J. A. Kessler, *PLoS One*, 2017, **12**, e0190150.
40 M. D. Jorgenen and J. Chmielewski, *Chem. Commun.*, 2022, **58**, 11625–11636.
41 N. Mehrban, B. Zhu, F. Tamagnini, F. I. Young, A. Wasmuth, K. L. Hudson, A. R. Thomson, M. A. Birchall, A. D. Randall, B. Song and D. N. Woolfson, *ACS Biomater. Sci. Eng.*, 2015, **1**, 431–439.
42 M. Reches and E. Gazit, *Science*, 2003, **300**, 625–627.
43 M. Reches and E. Gazit, *Nano Lett.*, 2004, **4**, 581–585.
44 Z. M. Yang, K. M. Xu, L. Wang, H. W. Gu, H. Wei, M. J. Zhang and B. Xu, *Chem. Commun.*, 2005, 4414–4416.
45 Z. M. Yang, H. W. Gu, Y. Zhang, L. Wang and B. Xu, *Chem. Commun.*, 2004, 208–210.
46 V. Jayawarna, M. Ali, T. A. Jowitt, A. F. Miller, A. Saiani, J. E. Gough and R. V. Ulijn, *Adv. Mater.*, 2006, **18**, 611–614.
47 Y. Wang, Q. Geng, Y. Zhang, L. Adler-Abramovich, X. Fan, D. Mei, E. Gazit and K. Tao, *J. Colloid Interface Sci.*, 2023, **636**, 113–133.
48 T. Liebmann, S. Rydholm, V. Akpe and H. Brismar, *BMC Biotechnol.*, 2007, **7**, 88.
49 H. Najafi, A. M. Tamaddon, S. Abolmaali, S. Borandeh and N. Azarpira, *Soft Matter*, 2021, **17**, 57–67.
50 G. Cheng, V. Castelletto, R. R. Jones, C. J. Connon and I. W. Hamley, *Soft Matter*, 2011, **7**, 1326–1333.
51 A. D. Martin, J. P. Wojciechowski, E. Y. Du, A. Rawal, H. Stefen, C. G. Au, L. Hou, C. G. Cranfield, T. Fath, L. M. Ittner and P. Thordarson, *Chem. Sci.*, 2020, **11**, 1375–1382.
52 S. Abdelrahman, R. Ge, H. H. Susapto, Y. Liu, F. Samkari, M. Moretti, X. Liu, R. Hoehndorf, A.-H. Emwas, M. Jaremko, R. H. Rawas and C. A. E. Hauser, *ACS Nano*, 2023, **17**, 14508–14531.
53 J. D. Tang, C. Mura and K. J. Lampe, *J. Am. Chem. Soc.*, 2019, **141**, 4886–4899.
54 L. Lv, H. Liu, X. Chen and Z. Yang, *Colloids Surf., B*, 2013, **108**, 352–357.
55 L. Guo, J. Lan, J. Li, Y. Song, X. Wang, Y. Zhao and Y. Yuan, *J. Colloid Interface Sci.*, 2024, **659**, 385–396.
56 S. Pan, S. Luo, S. Li, Y. Lai, Y. Geng, B. He and Z. Gu, *Chem. Commun.*, 2013, **49**, 8045–8047.
57 Y. Hu, H. Wang, J. Wang, S. Wang, W. Liao, Y. Yang, Y. Zhang, D. Kong and Z. Yang, *Org. Biomol. Chem.*, 2010, **8**, 3267–3271.
58 S. Nie, C. Ren, X. Liang, H. Cai, H. Sun, F. Liu, K. Ji, Y. Wang and Q. Liu, *Cells*, 2022, **11**, 3089.
59 L. A. Castillo Diaz, M. Elsawy, A. Saiani, J. E. Gough and A. F. Miller, *J. Tissue Eng.*, 2016, **7**, 2041731416649789.
60 E. Lingard, S. Dong, A. Hoyle, A. Hales, E. Skaria, C. Lawless, I. Taylor-Hearn, S. Saadati, Q. Chu, A. F. Miller, M. Domingos, A. Saiani, J. Swift and A. P. Gilmore, *Biomater. Adv.*, 2024, **160**, 213847.
61 H. C. Clough, M. O'Brien, X. Zhu, A. F. Miller, A. Saiani and O. Tsigkou, *Mater. Sci. Eng., C*, 2021, **127**, 112200.
62 N. J. Treacy, S. Clerkin, J. L. Davis, C. Kennedy, A. F. Miller, A. Saiani, J. K. Wychowaniec, D. F. Brougham and J. Crean, *Bioact. Mater.*, 2023, **21**, 142–156.
63 I. Bang, *Biochem. Z.*, 1910, **26**, 293–311.
64 M. Godoy-Gallardo, M. Merino-Gómez, L. C. Matiz, M. A. Mateos-Timoneda, F. J. Gil and R. A. Perez, *ACS Biomater. Sci. Eng.*, 2023, **9**, 40–61.
65 S. Ziane, S. Schlaubitz, S. Miraux, A. Patwa, C. Lalande, I. Bilem, S. Lepreux, B. Rousseau, J. F. Le Meins, L. Latxague, P. Barthélémy and O. Chassande, *Eur. Cells Mater.*, 2012, **23**, 147–160.
66 L. Latxague, M. A. Ramin, A. Appavoo, P. Berto, M. Maisani, C. Ehret, O. Chassande and P. Barthélémy, *Angew. Chem., Int. Ed.*, 2015, **54**, 4517–4521.
67 L. A. Estroff and A. D. Hamilton, *Chem. Rev.*, 2004, **104**, 1201–1218.
68 R. E. Kieltyka, A. C. H. Pape, L. Albertazzi, Y. Nakano, M. M. C. Bastings, I. K. Voets, P. Y. W. Dankers and E. W. Meijer, *J. Am. Chem. Soc.*, 2013, **135**, 11159–11164.
69 S. I. S. Hendrikse, S. P. W. Wijnands, R. P. M. Lafleur, M. J. Pouderoijen, H. M. Janssen, P. Y. W. Dankers and E. W. Meijer, *Chem. Commun.*, 2017, **53**, 2279–2282.
70 M. Diba, S. Spaans, S. I. S. Hendrikse, M. M. C. Bastings, M. J. G. Schotman, J. F. Van Sprang, D. J. Wu, F. J. M. Hoeben, H. M. Janssen and P. Y. W. Dankers, *Adv. Mater.*, 2021, **33**, 2008111.
71 M. J. Meunier, *Ann. Chim. Phys.*, 1891, **22**, 412.

72 A. Chalard, L. Vaysse, P. Joseph, L. Malaquin, S. Souleille, B. Lonetti, J.-C. Sol, I. Loubinoux and J. Fitremann, *ACS Appl. Mater. Interfaces*, 2018, **10**, 17004–17017.
73 K. K. Bayram, J. Fitremann, A. Bayram, Z. Yılmaz, E. Mehmetbeyoğlu, Y. Özkul and M. Rassoulzadegan, *Processes*, 2021, **9**, 716.
74 N. Kasmi, L. Pieruccioni, E. Pitot, I. Fourquaux, A. Wodrinski, L. Gibot and J. Fitremann, *J. Mater. Chem. B*, 2025, **13**, 4386–4405.
75 B. O. Okesola, V. M. P. Vieira, D. J. Cornwell, N. K. Whitelaw and D. K. Smith, *Soft Matter*, 2015, **11**, 4768–4787.
76 B. O. Okesola and D. K. Smith, *Chem. Commun.*, 2013, **49**, 11164–11166.
77 V. M. P. Vieira, A. C. Lima, M. de Jong and D. K. Smith, *Chem. – Eur. J.*, 2018, **24**, 14849–15125.
78 C. C. Piras, A. G. Kay, P. G. Genever, J. Fitremann and D. K. Smith, *Chem. Sci.*, 2022, **13**, 1972–1981.
79 C. Tangsombun, A. Simpson, R. L. Charlton, L. E. Sabin, P. G. Genever and D. K. Smith, *Angew. Chem., Int. Ed.*, 2026, **65**, e23454.
80 X. Li, Y. Kuang, J. Shi, Y. Gao, H.-C. Lin and B. Xu, *J. Am. Chem. Soc.*, 2011, **133**, 17513–17518.
81 D. Wu, J. Zhou, J. Shi, X. Du and B. Xu, *Chem. Commun.*, 2014, **50**, 1992–1994.
82 X. Du, J. Zhou, O. Guvench, F. O. Sangiorgi, X. Li, N. Zhou and B. Xu, *Bioconjugate Chem.*, 2014, **25**, 1031–1035.
83 W. Wang, H. Wang, C. Ren, J. Wang, M. Tan, J. Shen, Z. Yang, P. G. Wang and L. Wang, *Carbohydr. Res.*, 2011, **346**, 1013–1017.
84 S. K. Talloj, B. Cheng, J.-P. Weng and H. C. Lin, *ACS Appl. Mater. Interfaces*, 2018, **10**, 15079–15087.
85 V. I. B. Castro, A. R. Araújo, F. Duarte, A. Sousa-Franco, R. L. Reis, I. Pashkuleva and R. A. Pires, *ACS Appl. Mater. Interfaces*, 2023, **15**, 29998–30007.
86 S. Bhowmik, B. Baral, T. Rit, H. C. Jha and A. K. Das, *Nanoscale*, 2024, **16**, 13613–13626.
87 S. Cantekin, T. F. A. de Greef and A. R. A. Palmans, *Chem. Soc. Rev.*, 2012, **41**, 6125–6137.
88 S. Varela-Aramburu, G. Morgese, L. Su, S. M. C. Schoenmakers, M. Perrone, L. Leanza, C. Perego, G. M. Pavan, A. R. A. Palmans and E. W. Meijer, *Biomacromolecules*, 2020, **21**, 4105–4115.
89 S. Hafeez, F. R. Passanha, A. J. Feliciano, F. A. A. Ruiter, A. Malheiro, R. P. M. Lafleur, N. M. Matsumoto, C. van Blitterswijk, L. Moroni, P. Wieringa, V. L. S. LaPointe and M. B. Baker, *Biomater. Sci.*, 2022, **10**, 4740.
90 R. van Lommel, L. A. J. Rutgeerts, W. M. De Borggraeve, F. De Proft and M. Alonso, *ChemPlusChem*, 2020, **85**, 267–276.
91 J. Liu, Y. Zhang, K. van Dongen, C. Kennedy, M. J. G. Schotman, P. P. Marín San Román, C. Storm, P. Y. W. Dankers and R. P. Sijbesma, *Biomacromolecules*, 2023, **24**, 2447–2458.
92 A. R. Hirst and D. K. Smith, *Chem. – Eur. J.*, 2005, **11**, 5496–5508.
93 L. E. Buerkle and S. J. Rowan, *Chem. Soc. Rev.*, 2012, **41**, 6089–6102.
94 M. Zhou, A. M. Smith, A. K. Das, N. W. Hodson, R. F. Collins, R. V. Ulijn and J. E. Gough, *Biomaterials*, 2009, **30**, 2523–2530.
95 J. P. Jung, A. K. Nagaraj, E. K. Fox, J. S. Rudra, J. M. Devgun and J. H. Collier, *Biomaterials*, 2009, **30**, 2400–2410.
96 R. M. Shah, N. A. Shah, M. M. Del Rosario Lim, C. Hsieh, G. Nuber and S. I. Stupp, *Proc. Natl. Acad. Sci. U. S. A.*, 2010, **107**, 3293–3298.
97 J. Li, X. Ma, D. Wu, Z. Su, H. Su, Z. Liu, Y. Chen and B. Yu, *ACS Appl. Polym. Mater.*, 2024, **6**, 1929–1943.
98 S. Bhowmik, A. Acharyya and A. K. Das, *ACS Appl. Bio Mater.*, 2025, **8**, 3983–3994.
99 L. Rijns, M. J. Hagelaars, J. J. B. van der Tol, S. Loerakker, C. V. C. Bouten and P. Y. W. Dankers, *Adv. Mater.*, 2024, **36**, 2300873.
100 D. Bairagi, P. Biswas, K. Basu, S. Hazra, D. Hermida-Merino, D. K. Sinha, I. W. Hamley and A. Banerjee, *ACS Appl. Bio Mater.*, 2019, **2**, 5235–5244.
101 C. O. Crosby, B. Stern, N. Kalkunte, S. Pedahzur, S. Ramesh and J. Zoldan, *Rev. Chem. Eng.*, 2020, **38**, 347–361.
102 S. Panja, B. Dietrich, A. J. Smith, A. Seddon and D. J. Adams, *ChemSystemsChem*, 2022, **4**, e202200008.
103 B. O. Okesola, Y. Wu, B. Derkus, S. Gani, D. Wu, D. Knani, D. K. Smith, D. J. Adams and A. Mata, *Chem. Mater.*, 2019, **31**, 7883–7897.
104 L. R. Smith, S. Cho and D. E. Discher, *Physiology*, 2017, **33**, 16–25.
105 T. Luo, B. Tan, L. Zhu, Y. Wang and J. A. Liao, *Front. Bioeng. Biotechnol.*, 2022, **10**, 817391.
106 E. V. Alakpa, V. Jayawarna, A. Lampel, K. V. Burgess, C. C. West, S. C. J. Bakker, S. Roy, N. Javid, S. Fleming, D. A. Lamprou, J. Yang, A. Miller, A. J. Urquhart, P. W. J. Frederix, N. T. Hunt, B. Péault, R. V. Ulijn and M. J. Dalby, *Chem*, 2016, **1**, 298–319.
107 Y. Hu, W. Gao, F. Wu, H. Wu, B. He and J. He, *J. Mater. Chem. B*, 2016, **4**, 3504–3508.
108 J. He, Y. Hu, F. Wu, B. He and W. Gao, *J. Bionic Eng.*, 2018, **15**, 682–692.
109 M. Mohammed, T.-S. Lai and H.-C. Lin, *J. Mater. Chem. B*, 2021, **9**, 1676–1685.
110 B. F. Lin, K. A. Megley, N. Viswanathan, D. V. Krogstad, L. B. Drews, M. J. Kade, Y. Qian and M. V. Tirrell, *J. Mater. Chem. B*, 2012, **22**, 19447–19454.
111 J. M. Godbe, R. Freeman, L. F. Burbulla, J. Lewis, D. Krainc and S. I. Stupp, *ACS Biomater. Sci. Eng.*, 2020, **6**, 1196–1207.
112 B. Li, A. Çolak, J. Blass, M. Han, J. Zhang, Y. Zheng, Q. Jiang, R. Bennewitz and A. del Campo, *Mater. Today Bio*, 2022, **15**, 100323.
113 Z. Gong, S. E. Szczesny, S. R. Caliari, E. E. Charrier, O. Chaudhuri, X. Cao, Y. Lin, R. L. Mauck, P. A. Janmey, J. A. Burdick and V. B. Shenoy, *Proc. Natl. Acad. Sci. U. S. A.*, 2018, **115**, e2686–e2695.

114 L. Rijns, J. W. Peeters, S. I. S. Hendrikse, M. E. J. Vleugels, X. Lou, H. M. Janssen, E. W. Meijer and P. Y. W. Dankers, *Chem. Mater.*, 2023, **35**, 8203–8217.
115 Z. Álvarez, A. N. Kolberg-Edelbrock, I. R. Sasselli, J. A. Ortega, R. Qiu, Z. Syrgiannis, P. A. Mirau, F. Chen, S. M. Chin, S. Weigand, E. Kiskinis and S. I. Stupp, *Science*, 2021, **374**, 848–856.
116 Z. Álvarez, J. A. Ortega, K. Sato, I. R. Sasselli, A. N. Kolberg-Edelbrock, R. Qiu, K. A. Marshall, T. P. Nguyen, C. S. Smith, K. A. Quinlan, V. Papakis, Z. Syrgiannis, N. A. Sather, C. Musumeci, E. Engel, S. I. Stupp and E. Kiskinis, *Cell Stem Cell*, 2023, **30**, 219–238.
117 O. Chaudhuri, L. Gu, D. Klumpers, M. Darnell, S. A. Bencherif, J. C. Weaver, N. Huebsch, H. P. Lee, E. Lippens, G. N. Duda and D. J. Mooney, *Nat. Mater.*, 2016, **15**, 326–334.
118 S. Tang, H. Ma, H.-C. Tu, H.-R. Wang, P.-C. Lin and K. S. Anseth, *Adv. Sci.*, 2018, **5**, 1800638.
119 A. Elosegui-Artola, A. Gupta, A. J. Najibi, B. R. Seo, R. Garry, C. M. Tringides, I. de Lázaro, M. Darnell, W. Gu, Q. Zhou, D. A. Weitz, L. Mahadevan and D. J. Mooney, *Nat. Mater.*, 2023, **22**, 117–127.
120 D. S. W. Benoit, M. P. Schwartz, A. R. Durney and K. S. Anseth, *Nat. Mater.*, 2008, **7**, 816–823.
121 V. Jayawarna, S. M. Richardson, A. R. Hirst, N. W. Hodson, A. Saiani, J. E. Gough and R. V. Ulijn, *Acta Biomater.*, 2009, **5**, 934–943.
122 O. Yasa, O. Uysal, M. Sardan Ekiz, M. O. Guler and A. B. Tekinay, *J. Mater. Chem. B*, 2017, **5**, 4890–4900.
123 A. J. Keung, S. Kumar and D. V. Schaffer, *Annu. Rev. Cell Dev. Biol.*, 2010, **26**, 533–556.
124 W. L. Murphy, T. C. McDevitt and A. J. Engler, *Nat. Mater.*, 2014, **13**, 547–557.
125 D. K. Smith, *Chem. Soc. Rev.*, 2009, **38**, 684–694.
126 P. Duan, H. Cao, L. Zhang and M. Liu, *Soft Matter*, 2014, **10**, 5428–5448.
127 M. Melchionna, K. E. Styan and S. Marchesan, *Curr. Top. Med. Chem.*, 2016, **16**, 2009–2018.
128 Z. Luo, Y. Yue, Y. Zhang, X. Yuan, J. Gong, L. Wang, H. Bin, Z. Liu, Y. Sun, J. Liu, M. Hu and J. Zheng, *Biomaterials*, 2013, **34**, 4902–4913.
129 W. K. Restu, S. Yamamoto, Y. Nishida, H. Ienaga, T. Aoi and T. Maruyama, *Mater. Sci. Eng., C*, 2020, **111**, 110746.
130 S. Marchesan, C. D. Easton, K. Styan, L. Waddington, F. Kushkaki, L. Goodall, K. McLean, J. Forsythe and P. G. Hartley, *Nanoscale*, 2014, **6**, 5172–5180.
131 G. F. Liu, D. Zhang and C. L. Feng, *Angew. Chem., Int. Ed.*, 2014, **53**, 7789–7793.
132 J. Liu, F. Yuan, X. Ma, D.-i. Y. Auphedeous, C. Zhao, C. Liu, C. Shen and C. Feng, *Angew. Chem., Int. Ed.*, 2018, **57**, 6475–6479.
133 S. He, Y. Zhang, C. Zhao, X. Wang, S. Baddi, B. Wu, X. Dou and C. Feng, *Chem. – Eur. J.*, 2023, **29**, e202202735.
134 X. Dou, B. Wu, J. Liu, C. Zhao, M. Qin, Z. Wang, H. Schönherr and C. Feng, *ACS Appl. Mater. Interfaces*, 2019, **11**, 38568–38577.
135 P. Li, Q. Jin, K. Zeng, C. Niu, Q. Xie, T. Dong, Z. Huang, X. Dou and C. Feng, *Mater. Today Bio*, 2024, **25**, 100971.
136 Y. Zhang, H. Zheng, Y. Zhao, C. Du, J. Zhang, J. Liu, S. Jiang, Y. Wei and C. Feng, *ACS Nano*, 2025, **19**, 20564–20577.
137 C. Xing, W. Hou, L. Gao, X. Dou, Q. Zhao, T. Ni, P. Xu, B. Wu, H. Wu and C. Feng, *ACS Appl. Mater. Interfaces*, 2025, **17**, 14983–14994.
138 Y. Zhang, Y. Chen, J. Li, J. Zhang, C.-L. Feng and J. Liu, *Soft Matter*, 2025, **21**, 8252–8256.
139 Y. Zhang, S. Ai, Z. Yu, L. Wang, H. Tao, B. Wang, D. Kong, Z. Yang and Y. Wang, *Adv. Funct. Mater.*, 2024, **34**, 2314607.
140 D. J. Cornwell and D. K. Smith, *Mater. Horiz.*, 2015, **2**, 279–293.
141 M. Ghosh, M. Halperin-Sternfeld, I. Grigoriants, J. Lee, K. T. Nam and L. Adler-Abramovich, *Biomacromolecules*, 2017, **18**, 3541–3550.
142 C. Gila-Vilchez, M. C. Mañas-Torres, O. D. García-García, A. Escribano-Huesca, L. Rodríguez-Arco, V. Carriel, I. Rodriguez, M. Alaminos, M. T. Lopez-Lopez and L. Álvarez de Cienfuegos, *ACS Appl. Polym. Mater.*, 2023, **5**, 2154–2165.
143 M. Maisani, S. Ziane, C. Ehret, L. Levesque, R. Siadous, J.-F. Le Meins, P. Chevallier, P. Barthélémy, H. De Oliveira, J. Amédée, D. Mantovani and O. Chassande, *J. Tissue Eng. Regener. Med.*, 2018, **12**, 1489–1500.
144 E. Radvar and H. S. Azevedo, *ACS Biomater. Sci. Eng.*, 2019, **5**, 4646–4656.
145 B. Derkus, B. O. Okesola, D. W. Barrett, M. D'Este, T. T. Chowdhury, D. Eglin and A. Mata, *Acta Biomater.*, 2020, **109**, 82–94.
146 J. Tan, M. Zhang, Z. Hai, C. Wu, J. Lin, W. Kuang, H. Tang, Y. Huang, X. Chen and G. Liang, *ACS Nano*, 2019, **13**, 5616–5622.
147 T. Fernández-Muiños, L. Recha-Sancho, P. López-Chicón, C. Castells-Sala, A. Mata and C. E. Semino, *Acta Biomater.*, 2015, **16**, 35–48.
148 N. Falcone, T. Shao, N. M. O. Andoy, R. Rashid, R. M. A. Sullan, X. Sun and H.-B. Kraatz, *Biomater. Sci.*, 2020, **8**, 5601–5614.
149 B. Cheng, Y. Yan, J. Qi, L. Deng, Z.-W. Shao, K.-Q. Zhang, B. Li, Z. Sun and X. Li, *ACS Appl. Mater. Interfaces*, 2018, **10**, 12474–12484.
150 P. Song, T. Han, Z. Wu, H. Fang, Y. Liu, W. Ying, X. Wang and C. Shen, *Adv. Sci.*, 2024, **11**, 2306577.
151 P. R. A. Chivers and D. K. Smith, *Nat. Rev. Mater.*, 2019, **4**, 463–478.
152 S. Khetan and J. A. Burdick, *Soft Matter*, 2011, **7**, 830–838.
153 C. C. Piras, P. Slavik and D. K. Smith, *Angew. Chem., Int. Ed.*, 2020, **59**, 853–859.
154 C. C. Piras and D. K. Smith, *Chem. – Eur. J.*, 2021, **27**, 14527–14534.
155 C. C. Piras, C. S. Mahon, P. G. Genever and D. K. Smith, *ACS Biomater. Sci. Eng.*, 2022, **8**, 1829–1840.
156 B. O. Okesola, S. K. Suravaram, A. Parkin and D. K. Smith, *Angew. Chem., Int. Ed.*, 2016, **55**, 183–187.

157 C. C. Piras, P. G. Genever and D. K. Smith, *Mater. Adv.*, 2022, **3**, 7966–7975.
158 Y. F. Tian, J. M. Devgun and J. H. Collier, *Soft Matter*, 2011, **7**, 6005–6011.
159 C. C. Piras, A. G. Kay, P. G. Genever and D. K. Smith, *Chem. Sci.*, 2021, **12**, 3958–3965.
160 D. Fan, U. Staufer and A. Accardo, *Bioengineering*, 2019, **6**, 113.
161 T.-C. Ho, C.-C. Chang, H.-P. Chan, T.-W. Chung, C.-W. Shu, K.-P. Chuang, T.-H. Duh, M.-H. Yang and Y.-C. Tyan, *Molecules*, 2022, **27**, 2902.
162 B. Dessane, R. Smirani, G. Bouguéon, T. Kauss, E. Ribot, R. Devillard, P. Barthélémy, A. Naveau and S. Crauste-Manciet, *Sci. Rep.*, 2020, **10**, 2850.
163 M. Godoy-Gallardo, M. Merino-Gómez, M. A. Mateos-Timoneda, U. Eckhard, F. J. Gil and R. A. Perez, *ACS Appl. Mater. Interfaces*, 2023, **15**, 29729–29742.
164 S. Hafeez, A. Aldana, H. Duimel, F. A. A. Ruiter, M. C. Decarli, V. Lapointe, C. van Blitterswijk, L. Moroni and M. B. Baker, *Adv. Mater.*, 2023, **35**, 2207053.
165 A. C. Farsheed, A. J. Thomas, B. H. Pogostin and J. D. Hartgerink, *Adv. Mater.*, 2023, **35**, 2210378.
166 S. Zhang, M. A. Greenfield, A. Mata, L. C. Palmer, R. Bitton, J. R. Mantei, C. Aparicio, M. Olvera de la Cruz and S. I. Stupp, *Nat. Mater.*, 2010, **9**, 594–601.
167 D. McDowall, M. Walker, M. Vassalli, M. Cantini, N. Khunti, J. C. Edwards-Gayle, N. Cowieson and D. J. Adams, *Chem. Commun.*, 2021, **57**, 8782–8785.
168 D. Ghosh, M. Walker, L. Matthews, C. Patterson, O. Dobre, M. Vassalli and D. J. Adams, *Small*, 2026, **22**, e13952.
169 A. Chalard, P. Joseph, S. Souleille, B. Lonetti, N. Saffon-Merceron, I. Loubinoux, L. Vaysse, L. Malaquin and J. Fitremann, *Nanoscale*, 2019, **11**, 15043–15056.
170 F. Andriamiseza, D. Bordignon, B. Payré, L. Vaysse and J. Fitremann, *J. Colloid Interface Sci.*, 2022, **617**, 156–170.
171 A. Chalard, M. Mauduit, S. Souleille, P. Joseph, L. Malaquin and J. Fitremann, *Addit. Manuf.*, 2020, **33**, 101162.
172 D. J. Cornwell, B. O. Okesola and D. K. Smith, *Angew. Chem., Int. Ed.*, 2014, **53**, 12461–12465.
173 P. R. A. Chivers and D. K. Smith, *Chem. Sci.*, 2017, **8**, 7218–7227.
174 N. Zhang, Y. Wang, J. Zhang, J. Guo and J. He, *Acta Biomater.*, 2021, **135**, 304–317.
175 Á. López–Acosta, P. R. A. Chivers, C. C. Piras, A. G. Kay, P. G. Genever and D. K. Smith, *ChemNanoMat*, 2024, **10**, e202400183.
176 C. Tangsombun, A. Simpson, P. G. Genever and D. K. Smith, *Adv. Healthcare Mater.*, 2025, **14**, 2405057.
177 V. I. B. Castro, S. Amorim, D. Caballero, C. M. Abreu, S. C. Kundu, R. L. Reis, I. Pashkuleva and R. A. Pires, *Biomater. Adv.*, 2025, **167**, 214091.
178 K. M. Hainline, F. Gu, J. F. Handley, Y. F. Tian, Y. Wu, L. de Wet, D. J. van der Griend and J. H. Collier, *Macromol. Biosci.*, 2019, **19**, 1800249.
179 S. Jones, J. C. Ashworth, M. Meakin, P. Collier, C. Probert, A. A. Ritchie, C. L. R. Merry and A. R. Grabowska, *In Vitro Models*, 2023, **2**, 99–111.
180 N. Zanna, S. Focaroli, A. Merlettini, L. Gentilucii, G. Teti, M. Falconi and C. Tomasini, *ACS Omega*, 2017, **2**, 2374–2381.
181 C. Tong, T. Liu, V. Saez Talens, W. E. M. Noteborn, T. H. Sharp, M. M. R. M. Hendrix, I. K. Voets, C. L. Mummery, V. V. Orlova and R. E. Kieltyka, *Biomacromolecules*, 2018, **19**, 1091–1099.
182 J. Raeburn, A. Z. Cardoso and D. J. Adams, *Chem. Soc. Rev.*, 2013, **42**, 5143–5156.
183 F. Tantakitti, J. Boekhoven, X. Wang, R. V. Kazantsev, T. Yu, J. Li, E. Zhuang, R. Zandi, J. H. Ortony, C. J. Newcomb, L. C. Palmer, G. S. Shekhawat, M. Olvera de la Cruz, G. C. Schatz and S. I. Stupp, *Nat. Mater.*, 2016, **15**, 469–476.
184 E. R. Draper and D. J. Adams, *Nat. Mater.*, 2024, **23**, 13–15.
185 S. Mohanty, S. Sen, P. Sharma and S. Roy, *Biomacromolecules*, 2024, **25**, 3271–3287.
186 M. Champeau, D. A. Heinze, T. N. Viana, E. Rodrigues de Souza, A. C. Chinellato and S. Titotto, *Adv. Funct. Mater.*, 2020, **30**, 1910606.
187 A. Nain, S. Chakraborty, N. Jain, S. Choudhury, S. Chattopadhyay, K. Chatterjee and S. Debnath, *Biomater. Sci.*, 2024, **12**, 3249–3272.
188 C. Yang, D. Li, Z. Liu, G. Hong, J. Zhang, D. Kong and Z. Yang, *J. Phys. Chem. B*, 2012, **116**, 633–638.
189 C. Ligorio, M. Martinez-Espuga, D. Laurenza, A. Hartley, C. B. Rodgers, A. M. Kotowska, D. J. Scurr, M. J. Dalby, P. Ordóñez-Morán and A. Mata, *J. Mater. Chem. B*, 2024, **12**, 11939–11952.
190 M. He, J. Li, S. Tan, R. Wang and Y. Zhang, *J. Am. Chem. Soc.*, 2013, **135**, 18718–18721.
191 A. K. Das, I. Maity, H. S. Parmar, T. O. McDonald and M. Konda, *Biomacromolecules*, 2015, **16**, 1157–1168.
192 A. Sharko, D. Livitz, S. De Piccoli, K. J. M. Bishop and T. M. Hermans, *Chem. Rev.*, 2022, **122**, 11759–11777.
193 S. Bhowmik, T. Rit, Y. S. Sanghvi and A. K. Das, *Chem. – Eur. J.*, 2024, **30**, e202402687.
194 A. N. Shy, B. J. Kim and B. Xu, *Matter*, 2019, **1**, 1127–1147.
195 H. Wang, Z. Feng and B. Xu, *Angew. Chem., Int. Ed.*, 2019, **58**, 10423–10432.
196 H. Wang, Z. Feng and B. Xu, *J. Am. Chem. Soc.*, 2019, **141**, 7271–7274.
197 J. Guo, F. Wang, Y. Huang, H. He, W. Tan, M. Yi, E. H. Egelman and B. Xu, *Nat. Nanotechnol.*, 2023, **18**, 1094–1104.

